

# O modelowaniu zamarzania przechłodzonych kropelek wody w chmurach

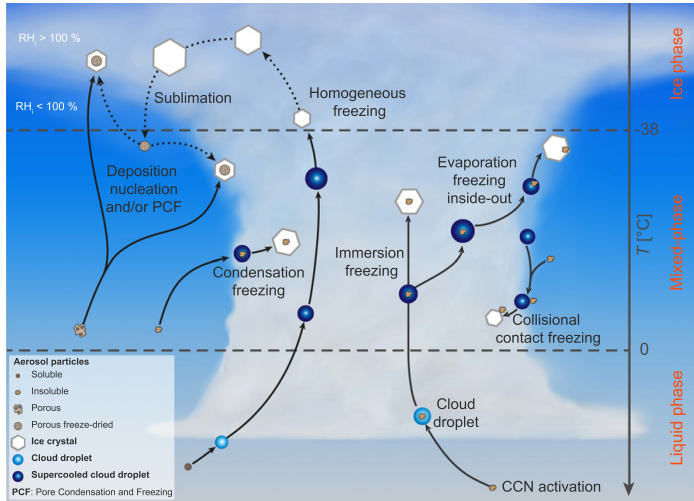
S. Arabas<sup>1</sup>, J.H. Curtis<sup>2</sup>, A. Fridlind<sup>3</sup>, D.A Knopf<sup>4</sup>, M. West<sup>2</sup> & N. Riemer<sup>2</sup>



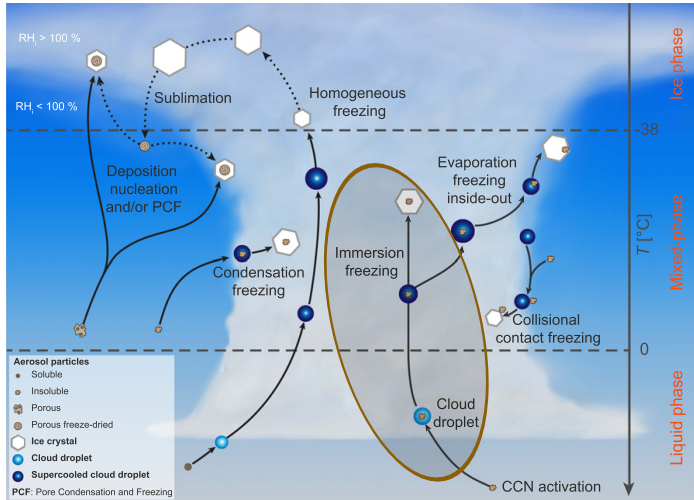
finansowanie:



Seminarium Wydziału Fizyki i Informatyki Stosowanej AGH, 26.V 2023 r.



Kanji et al. 2017, graphics F. Mahrt, <https://doi.org/10.1175/AMSMONOGRAPHS-D-16-0006.1>



Kanji et al. 2017, graphics F. Mahrt, <https://doi.org/10.1175/AMSMONOGRAPHS-D-16-0006.1>

## RESEARCH ARTICLE

10.1002/2016JD025251

### Key Points:

- Very ice active Snomax protein aggregates are fragile and their ice nucleation ability decreases over months of freezer storage
- Partitioning of ice active protein aggregates into the immersion oil reduces the droplet's measured freezing temperature

© 2016 American Geophysical Union. All Rights Reserved.

## The unstable ice nucleation properties of Snomax® bacterial particles

Michael Polen<sup>1</sup>, Emily Lawlis<sup>1</sup>, and Ryan C. Sullivan<sup>1</sup>

<sup>1</sup>Center for Atmospheric Particle Studies, Carnegie Mellon University, Pittsburgh, Pennsylvania, USA

---

**Abstract** Snomax® is often used as a surrogate for biological ice nucleating particles (INPs) and has recently been proposed as an INP standard for evaluating ice nucleation methods. We have found the immersion freezing properties of Snomax particles to be substantially unstable, observing a loss of ice nucleation ability

## RESEARCH ARTICLE

10.1002/2016JD025251

### Key Points:

- Very ice active Snomax protein aggregates are fragile and their ice nucleation ability decreases over months of freezer storage
- Partitioning of ice active protein aggregates into the immersion oil reduces the droplet's measured freezing temperature

## The unstable ice nucleation properties of Snomax® bacterial particles

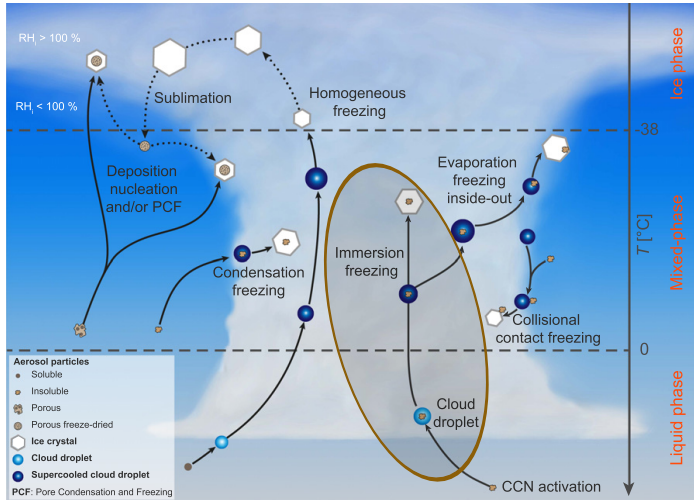
Michael Polen<sup>1</sup>, Emily Lawlis<sup>1</sup>, and Ryan C. Sullivan<sup>1</sup>

<sup>1</sup>Center for Atmospheric Particle Studies, Carnegie Mellon University, Pittsburgh, Pennsylvania, USA

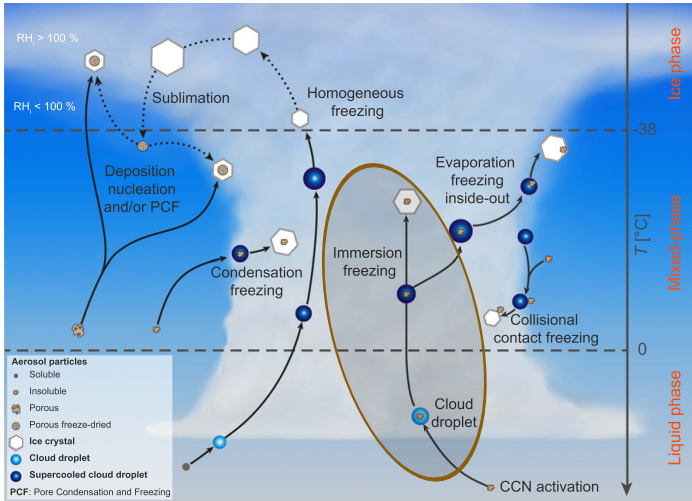
**Abstract** Snomax® is often used as a surrogate for biological ice nucleating particles (INPs) and has recently been proposed as an INP standard for evaluating ice nucleation methods. We have found the immersion freezing properties of Snomax particles to be substantially unstable, observing a loss of ice nucleation ability



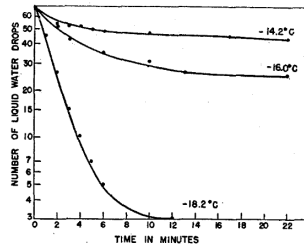
<https://www.reuters.com/markets/commodities/making-snow-stick-wind-challenges-winter-games-slope-makers-2021-11-29/>



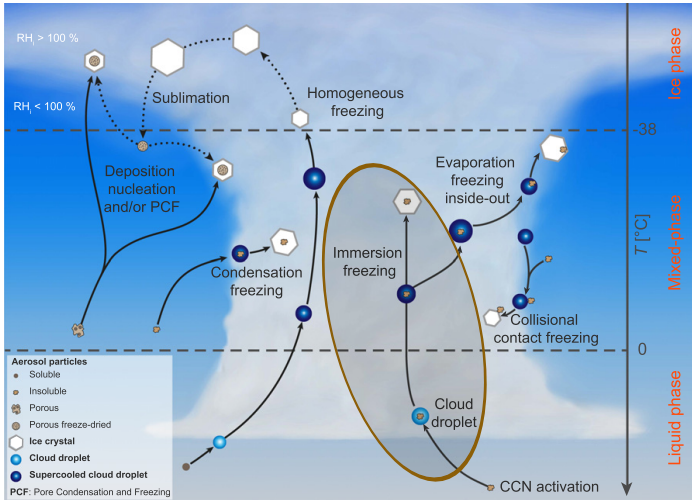
Kanji et al. 2017, graphics F. Mahrt, <https://doi.org/10.1175/AMSMONOGRAPHS-D-16-0006.1>



Vonnegut 1948 (J. Colloid Sci.)

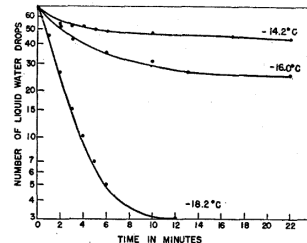


Fraction of water drops remaining unfrozen as a function of time.



Kanji et al. 2017, graphics F. Mahrt, <https://doi.org/10.1175/AMSMONOGRAPHS-D-16-0006.1>

### Vonnegut 1948 (J. Colloid Sci.)



Fraction of water drops remaining unfrozen as a function of time.

### Vali 2014 (ACP)

*"Interpretations of the experimental results face considerable difficulties ... two separate ways of interpreting the same observations; one assigned primacy to time the other emphasized the temperature-dependent impacts of the impurities ... dichotomy – the stochastic and singular models"*

# Heterogeneous Nucleations is a Stochastic Process

by

J. S. MARSHALL

McGill University, Montreal, Canad.

*Presented at the International Congress on the Physics of Clouds (Hailstorms)  
at Verona 9-13 August 1960.*

[http://cma.entepra.it/Astro2\\_sito/doc/Nubila\\_1\\_1961.pdf](http://cma.entepra.it/Astro2_sito/doc/Nubila_1_1961.pdf)

theory (in modern notation)

(Bigg '53, Langham & Mason '58, Carte '59, Marshall '61)

theory (in modern notation)

(Bigg '53, Langham & Mason '58, Carte '59, Marshall '61)

Poisson counting process with rate  $r$ :

$$P^*(k \text{ events in time } t) = \frac{(rt)^k \exp(-rt)}{k!}$$

$$P(\text{one or more events in time } t) = 1 - P^*(k = 0, t)$$

$$\ln(1 - P) = -rt$$

theory (in modern notation)

(Bigg '53, Langham & Mason '58, Carte '59, Marshall '61)

Poisson counting process with rate  $r$ :

$$P^*(k \text{ events in time } t) = \frac{(rt)^k \exp(-rt)}{k!}$$

$$P(\text{one or more events in time } t) = 1 - P^*(k=0, t)$$

$$\ln(1 - P) = -rt$$

introducing  $J_{\text{het}}(T)$ ,  $T(t)$  and INP surface  $A$ :

$$\ln(1 - P(A, t)) = -A \underbrace{\int_0^t J_{\text{het}}(T(t')) dt'}_{n_s(T)}$$

theory (in modern notation)

(Bigg '53, Langham & Mason '58, Carte '59, Marshall '61)

Poisson counting process with rate  $r$ :

$$P^*(k \text{ events in time } t) = \frac{(rt)^k \exp(-rt)}{k!}$$

$$P(\text{one or more events in time } t) = 1 - P^*(k=0, t)$$

$$\ln(1 - P) = -rt$$

introducing  $J_{\text{het}}(T)$ ,  $T(t)$  and INP surface  $A$ :

$$\ln(1 - P(A, t)) = -A \underbrace{\int_0^t J_{\text{het}}(T(t')) dt'}_{n_s(T)}$$

experimental fits (same data, both exp-linear):

INAS (Niemand et al.):  $n_s(T) = \dots$

theory (in modern notation)

(Bigg '53, Langham & Mason '58, Carte '59, Marshall '61)

Poisson counting process with rate  $r$ :

$$P^*(k \text{ events in time } t) = \frac{(rt)^k \exp(-rt)}{k!}$$

$$P(\text{one or more events in time } t) = 1 - P^*(k=0, t)$$

$$\ln(1 - P) = -rt$$

introducing  $J_{\text{het}}(T)$ ,  $T(t)$  and INP surface  $A$ :

$$\ln(1 - P(A, t)) = -A \underbrace{\int_0^t J_{\text{het}}(T(t')) dt'}_{n_s(T)}$$

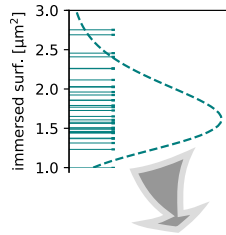
experimental fits (same data, both exp-linear):

INAS (Niemand et al.):  $n_s(T) = \dots$

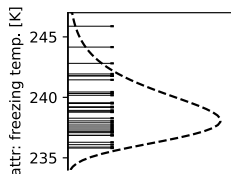
CNT/ABIFM (Knopf et al.):  $J_{\text{het}}(a_w(T)) = \dots$

## particle attribute sampling

**random** sampling of immersed surface for each particle

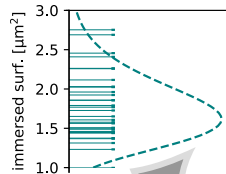


**random** sampling of freezing temperatures  
(conditional distribution for a given surface)

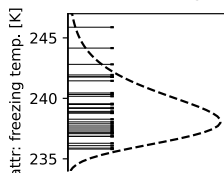


## particle attribute sampling

random sampling of immersed surface for each particle



random sampling of freezing temperatures  
(conditional distribution for a given surface)



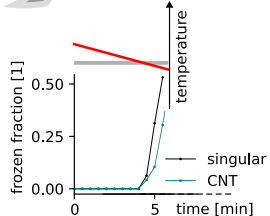
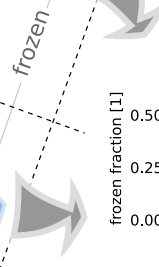
## particle dynamics

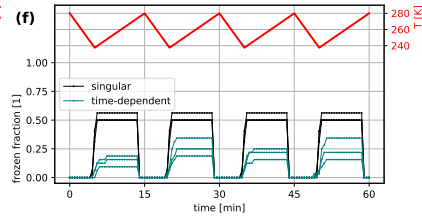
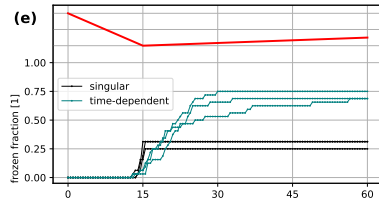
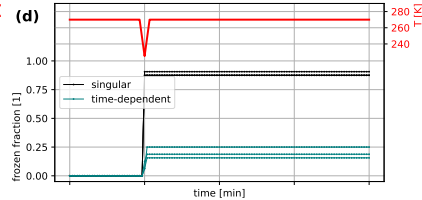
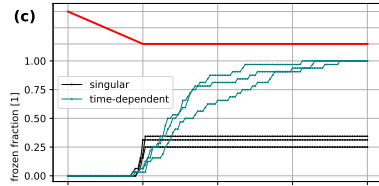
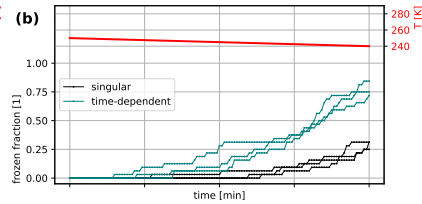
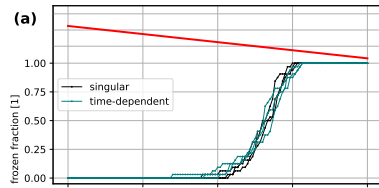
(discrete time Markov chain)

$P_i = J_S(T) \cdot S_i \cdot \Delta t$   
**probability of transition**  
in each timestep

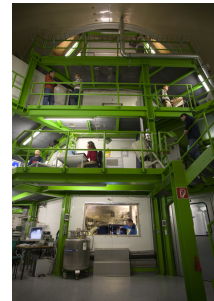
CNT  
singular

(finite state machine)  
**deterministic transition**  
if  $T$  falls below  $T_f$





# AIDA @ KIT



(<https://www.imk-aaf.kit.edu/73.php>, photo: KIT/Ottmar Möhler)

AIDA cooling rate:  $0.5 \text{ } K/min$

theory (in modern notation)

(Bigg '53, Langham & Mason '58, Carte '59, Marshall '61)

Poisson counting process with rate  $r$ :

$$P^*(k \text{ events in time } t) = \frac{(rt)^k \exp(-rt)}{k!}$$

$$P(\text{one or more events in time } t) = 1 - P^*(k=0, t)$$

$$\ln(1 - P) = -rt$$

introducing  $J_{\text{het}}(T)$ ,  $T(t)$  and INP surface  $A$ :

$$\ln(1 - P(A, t)) = -A \underbrace{\int_0^t J_{\text{het}}(T(t')) dt'}_{n_s(T)}$$

experimental fits (same data, both exp-linear):

INAS (Niemand et al.):  $n_s(T) = \dots$

CNT/ABIFM (Knopf et al.):  $J_{\text{het}}(a_w(T)) = \dots$

## theory (in modern notation)

(Bigg '53, Langham & Mason '58, Carte '59, Marshall '61)

Poisson counting process with rate  $r$ :

$$P^*(k \text{ events in time } t) = \frac{(rt)^k \exp(-rt)}{k!}$$

$$P(\text{one or more events in time } t) = 1 - P^*(k=0, t)$$

$$\ln(1 - P) = -rt$$

introducing  $J_{\text{het}}(T)$ ,  $T(t)$  and INP surface  $A$ :

$$\ln(1 - P(A, t)) = -A \underbrace{\int_0^t J_{\text{het}}(T(t')) dt'}_{n_s(T)}$$

experimental fits (same data, both exp-linear):

INAS (Niemand et al.):  $n_s(T) = \dots$

CNT/ABIFM (Knopf et al.):  $J_{\text{het}}(a_w(T)) = \dots$

for a constant cooling rate  $c = dT/dt$ :

$$\ln(1 - P(A, t)) = -\frac{A}{c} \int_{T_0}^{T_0 + ct} J_{\text{het}}(T') dT' = -A \cdot I(T)$$

## theory (in modern notation)

(Bigg '53, Langham & Mason '58, Carte '59, Marshall '61)

Poisson counting process with rate  $r$ :

$$P^*(k \text{ events in time } t) = \frac{(rt)^k \exp(-rt)}{k!}$$

$$P(\text{one or more events in time } t) = 1 - P^*(k=0, t)$$

$$\ln(1 - P) = -rt$$

introducing  $J_{\text{het}}(T)$ ,  $T(t)$  and INP surface  $A$ :

$$\ln(1 - P(A, t)) = -A \underbrace{\int_0^t J_{\text{het}}(T(t')) dt'}_{n_s(T)}$$

experimental fits (same data, both exp-linear):

INAS (Niemand et al.):  $n_s(T) = \dots$

CNT/ABIFM (Knopf et al.):  $J_{\text{het}}(a_w(T)) = \dots$

for a constant cooling rate  $c = dT/dt$ :

$$\ln(1 - P(A, t)) = -\frac{A}{c} \int_{T_0}^{T_0 + ct} J_{\text{het}}(T') dT' = -A \cdot I(T)$$

$$\frac{dn_s(T)}{dT} = a \cdot n_s(T) = -\frac{1}{c} J_{\text{het}}(T)$$

theory (in modern notation)

(Bigg '53, Langham & Mason '58, Carte '59, Marshall '61)

Poisson counting process with rate  $r$ :

$$P^*(k \text{ events in time } t) = \frac{(rt)^k \exp(-rt)}{k!}$$

$$P(\text{one or more events in time } t) = 1 - P^*(k = 0, t)$$

$$\ln(1 - P) = -rt$$

introducing  $J_{\text{het}}(T)$ ,  $T(t)$  and INP surface  $A$ :

$$\ln(1 - P(A, t)) = -A \int_0^t J_{\text{het}}(T(t')) dt'$$

experimental fits (same data, both exp-linear):

INAS (Niemand et al.):  $n_s(T) = \dots$

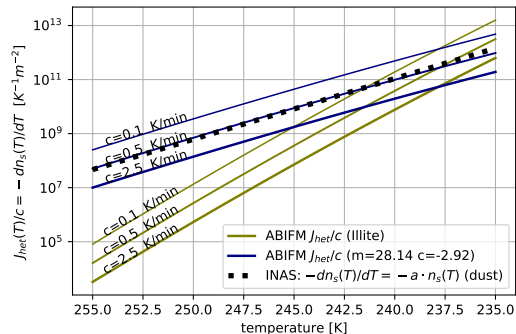
CNT/ABIFM (Knopf et al.):  $J_{\text{het}}(a_w(T)) = \dots$

for a constant cooling rate  $c = dT/dt$ :

$$\ln(1 - P(A, t)) = -\frac{A}{c} \int_{T_0}^{T_0 + ct} J_{\text{het}}(T') dT' = -A \cdot I(T)$$

$$\frac{dn_s(T)}{dT} = a \cdot n_s(T) = -\frac{1}{\zeta} J_{\text{het}}(T)$$

### experimental fits



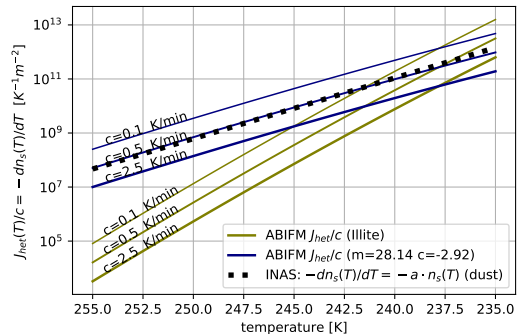
for a constant cooling rate  $c = dT/dt$ :

$$\ln(1 - P(A, t)) = -\frac{A}{c} \int_{T_0}^{T_0 + ct} J_{\text{het}}(T') dT' = -A \cdot I(T)$$

$$\frac{dn_s(T)}{dT} = a \cdot n_s(T) = -\frac{1}{c} J_{\text{het}}(T)$$

### experimental fits

?!



Shima, Sato, Hashimoto & Misumi 2020 (GMD):

*Predicting the morphology of ice particles in deep convection using the super-droplet method*

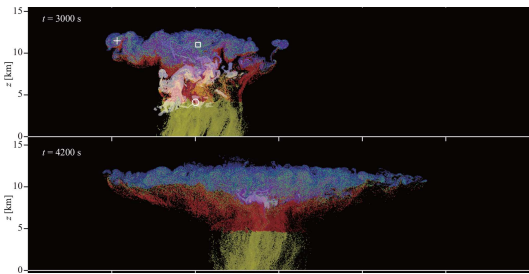
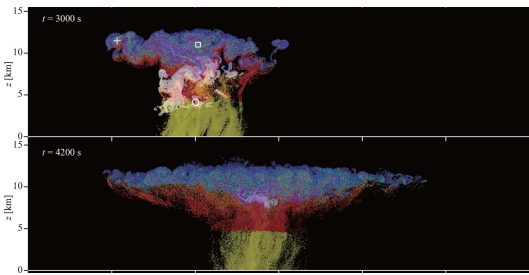


Figure 1. Typical realization of CTRL cloud spatial structures at  $t = 2040, 2460, 3000, 4200$ , and  $5400\text{ s}$ . The mixing ratio of cloud water, rainwater, cloud ice, graupel, and snow aggregates are plotted in fading white, yellow, blue, red, and green, respectively. The symbols indicate examples of unrealistic predicted ice particles (Sects. 7.3 and 9.1). See also Movie 1 in the video supplement.



# Shima, Sato, Hashimoto & Misumi 2020 (GMD):

## Predicting the morphology of ice particles in deep convection using the super-droplet method



► Eulerian component: momentum, heat, moisture budget

**Figure 1.** Typical realization of CTRL cloud spatial structures at  $t = 2040, 2460, 3000, 4200$ , and  $5400\text{ s}$ . The mixing ratio of cloud water, rainwater, cloud ice, graupel, and snow aggregates are plotted in fading white, yellow, blue, red, and green, respectively. The symbols indicate examples of unrealistic predicted ice particles (Sects. 7.3 and 9.1). See also Movie 1 in the video supplement.



# Shima, Sato, Hashimoto & Misumi 2020 (GMD):

## Predicting the morphology of ice particles in deep convection using the super-droplet method

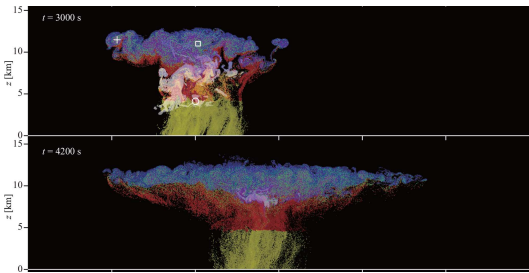


**Figure 1.** Typical realization of CTRL cloud spatial structures at  $t = 2040, 2460, 3000, 4200$ , and  $5400\text{ s}$ . The mixing ratio of cloud water, rainwater, cloud ice, graupel, and snow aggregates are plotted in fading white, yellow, blue, red, and green, respectively. The symbols indicate examples of unrealistic predicted ice particles (Sects. 7.3 and 9.1). See also Movie 1 in the video supplement.

- ▶ Eulerian component: momentum, heat, moisture budget
- ▶ Lagrangian component: super particles representing aerosol, water droplets, ice particles (porous spheroids)



# Shima, Sato, Hashimoto & Misumi 2020 (GMD):

## Predicting the morphology of ice particles in deep convection using the super-droplet method

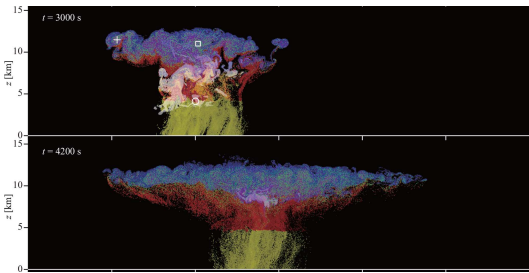


Figure 1. Typical realization of CTRL cloud spatial structures at  $t = 2040, 2460, 3000, 4200$ , and  $5400\text{ s}$ . The mixing ratio of cloud water, rainwater, cloud ice, graupel, and snow aggregates are plotted in fading white, yellow, blue, red, and green, respectively. The symbols indicate examples of unrealistic predicted ice particles (Sects. 7.3 and 9.1). See also Movie 1 in the video supplement.

- ▶ Eulerian component: momentum, heat, moisture budget
- ▶ Lagrangian component: super particles representing aerosol, water droplets, ice particles (porous spheroids)
- ▶ particle-resolved processes:
  - advection and sedimentation
  - homogeneous and immersion freezing (singular)
  - melting
  - condensation and evaporation (incl. CCN [de]activation)
  - deposition and sublimation
  - collisions (coalescence, riming, aggregation, washout)



Shima, Sato, Hashimoto & Misumi 2020 (GMD):

Predicting the morphology of ice particles in deep convection using the super-droplet method

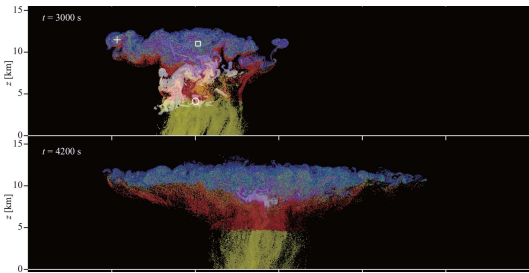


**Figure 1.** Typical realization of CTRL cloud spatial structures at  $t = 2040$ ,  $2460$ ,  $3000$ ,  $4200$ , and  $5400$  s. The mixing ratio of cloud water, rainwater, cloud ice, graupel, and snow aggregates are plotted in fading white, yellow, blue, red, and green, respectively. The symbols indicate examples of unrealistic predicted ice particles (Sects. 7.3 and 9.1). See also Movie 1 in the video supplement.



- ▶ Eulerian component: momentum, heat, moisture budget
  - ▶ Lagrangian component: super particles representing aerosol, water droplets, ice particles (porous spheroids)
  - ▶ particle-resolved processes:
    - advection and sedimentation
    - homogeneous and immersion freezing (singular)
    - melting
    - condensation and evaporation (incl. CCN [de]activation)
    - deposition and sublimation
    - collisions (coalescence, riming, aggregation, washout)
  - ▶ 2D Cb test case

# Shima, Sato, Hashimoto & Misumi 2020 (GMD):

## Predicting the morphology of ice particles in deep convection using the super-droplet method

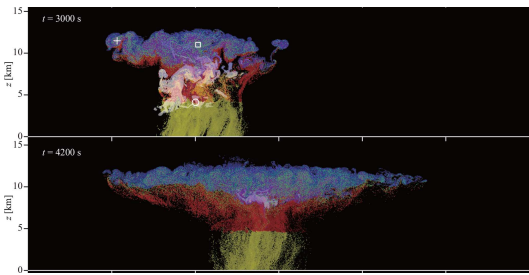
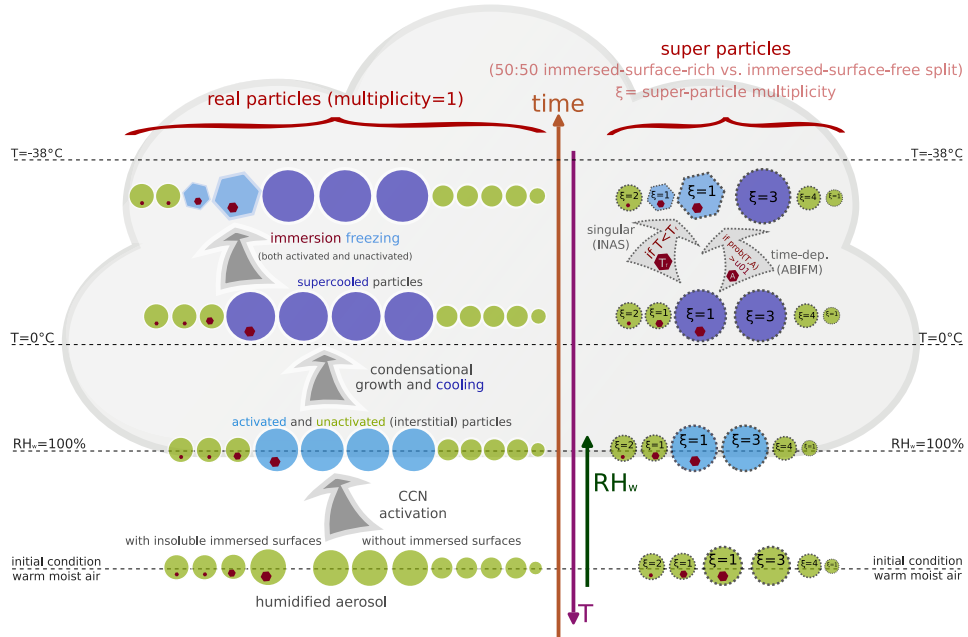


Figure 1. Typical realization of CTRL cloud spatial structures at  $t = 2040, 2460, 3000, 4200$ , and  $5400$  s. The mixing ratio of cloud water, rainwater, cloud ice, graupel, and snow aggregates are plotted in fading white, yellow, blue, red, and green, respectively. The symbols indicate examples of unrealistic predicted ice particles (Sects. 7.3 and 9.1). See also Movie 1 in the video supplement.



- ▶ Eulerian component: momentum, heat, moisture budget
- ▶ Lagrangian component: super particles representing aerosol, water droplets, ice particles (porous spheroids)
- ▶ particle-resolved processes:
  - advection and sedimentation
  - homogeneous and **immersion freezing (singular)**
  - melting
  - condensation and evaporation (incl. CCN [de]activation)
  - deposition and sublimation
  - collisions (coalescence, riming, aggregation, washout)
- ▶ 2D Cb test case



# new open-source HPC packages: Bartman et al. 2022 (JOSS)

PySDM 2.20

pip install PySDM

Released: Apr 21, 2023

Pythonic particle-based (super-droplet) warm-rain/aqueous-chemistry cloud microphysics package with box, parcel & 1D/2D prescribed-flow examples in Python, Julia and Matlab

Navigation

Project description

PySDM

Project links

Statistics

GitHub statistics:

- Stars: 40
- Forks: 21
- Open issues: 101
- Open PRs: 13

PySDM is a package for simulating the dynamics of population of particles. It is intended to serve as a building block for simulation systems modelling fluid flows involving a dispersed phase, with PySDM being responsible for representation of the dispersed phase. Currently, the development is focused on atmospheric cloud physics applications, in particular on modelling the dynamics of particles immersed in moist air using the particle-based (a.k.a. super-droplet) approach to represent aerosol/cloud/rain microphysics. The package features a Pythonic high-performance implementation of the Super-Droplet Method (SDM) Monte-Carlo algorithm for representing collisional growth (Shima et al. 2009), hence the name.

PyMPDATA 1.0.11

pip install PyMPDATA

Released: Apr 26, 2023

Numba-accelerated Pythonic implementation of MPDATA with examples in Python, Julia and Matlab

Navigation

Project description

PyMPDATA

Project links

Statistics

GitHub statistics:

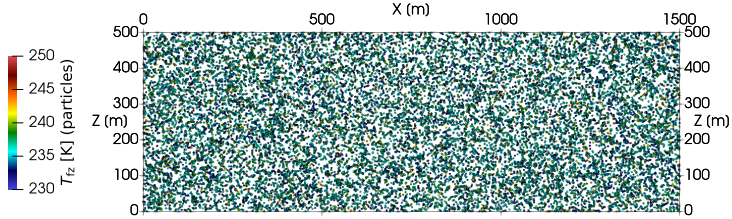
- Stars: 19
- Forks: 10
- Open issues: 25
- Open PRs: 3

PyMPDATA is a high-performance Numba-accelerated Pythonic implementation of the MPDATA algorithm of Smolarkiewicz et al. used in geophysical fluid dynamics and beyond. MPDATA numerically solves generalised transport equations - partial differential equations used to model conservation/balance laws, scalar-transport problems, convection-diffusion phenomena. As of the current version, PyMPDATA supports homogeneous transport in 1D, 2D and 3D using structured meshes, optionally generalised by employment of a Jacobian of coordinate transformation. PyMPDATA includes implementation of a set of MPDATA variants including the non-oscillatory option, infinite-gauge, divergent-flow, double-pass donor cell (DPDC) and third-order-term options. It also features support for integration of Fickian terms in advection-diffusion problems using the pseudo-transport velocity approach. In 2D and 3D problems, domain-decomposition is used for multi-threaded parallelism.

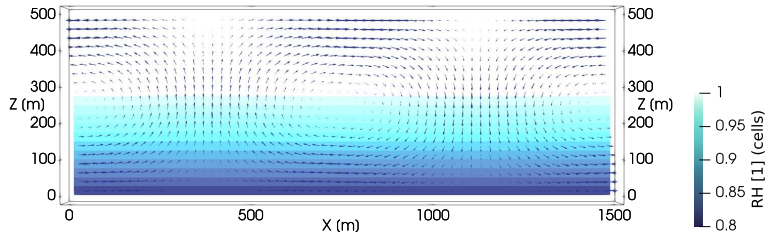
PyMPDATA is engineered purely in Python targeting both performance and usability, the latter encompassing research users', developers' and maintainers' perspectives. From researcher's perspective, PyMPDATA offers hassle-free

maintanance & development @ AGH: SA, Oleksii Bulenok, Kacper Derlatka

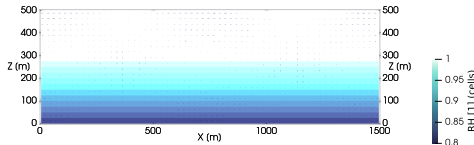
### Lagrangian component (PySDM)



### Eulerian component (PyMPDATA)



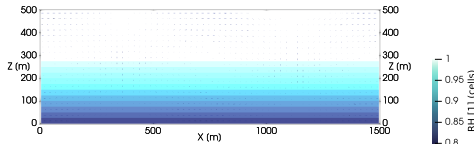
$w_{\max} \approx 1/3 \text{ m/s}$



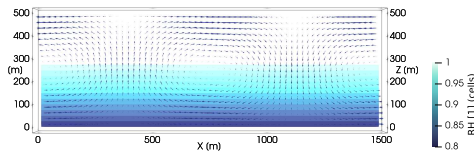
$w_{\max} \approx 1 \text{ m/s}$

$w_{\max} \approx 3 \text{ m/s}$

$w_{\max} \approx 1/3 \text{ m/s}$

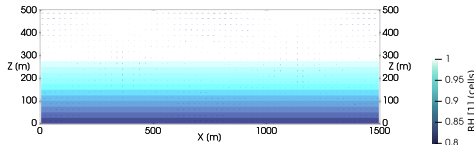


$w_{\max} \approx 1 \text{ m/s}$

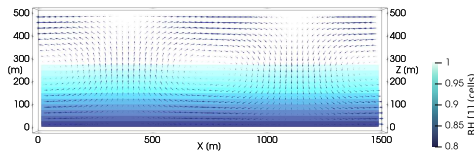


$w_{\max} \approx 3 \text{ m/s}$

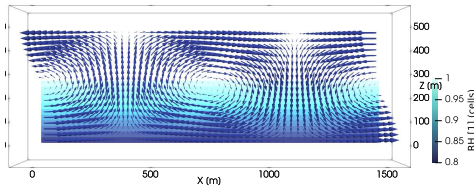
$w_{\max} \approx 1/3 \text{ m/s}$



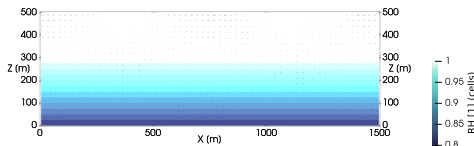
$w_{\max} \approx 1 \text{ m/s}$



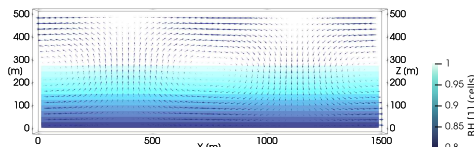
$w_{\max} \approx 3 \text{ m/s}$



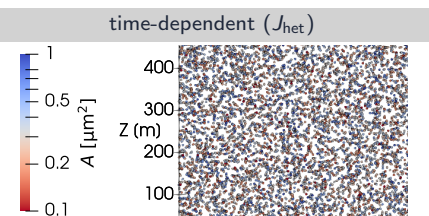
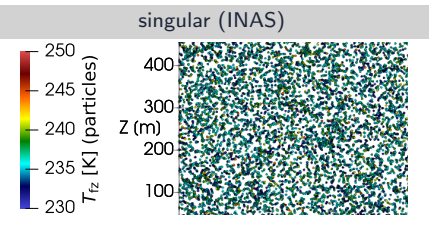
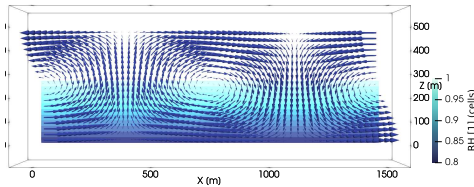
$w_{\max} \approx 1/3 \text{ m/s}$



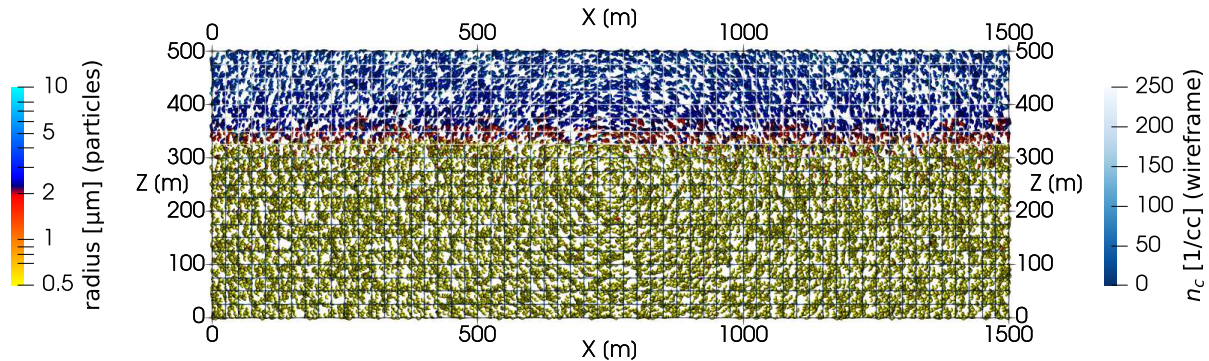
$w_{\max} \approx 1 \text{ m/s}$



$w_{\max} \approx 3 \text{ m/s}$

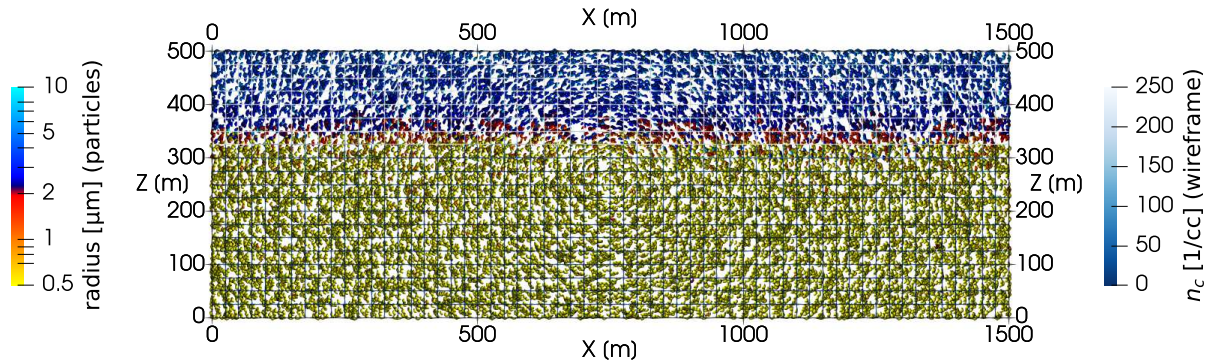


Time: 30 s (spin-up till 600.0 s)



16+16 super-particles/cell for INP-rich + INP-free particles  
 $N_{\text{aer}} = 300/\text{cc}$  (two-mode lognormal)    $N_{\text{INP}} = 150/L$  (lognormal,  $D_g = 0.74 \mu\text{m}$ ,  $\sigma_g = 2.55$ )  
spin-up = freezing off; subsequently frozen particles act as tracers

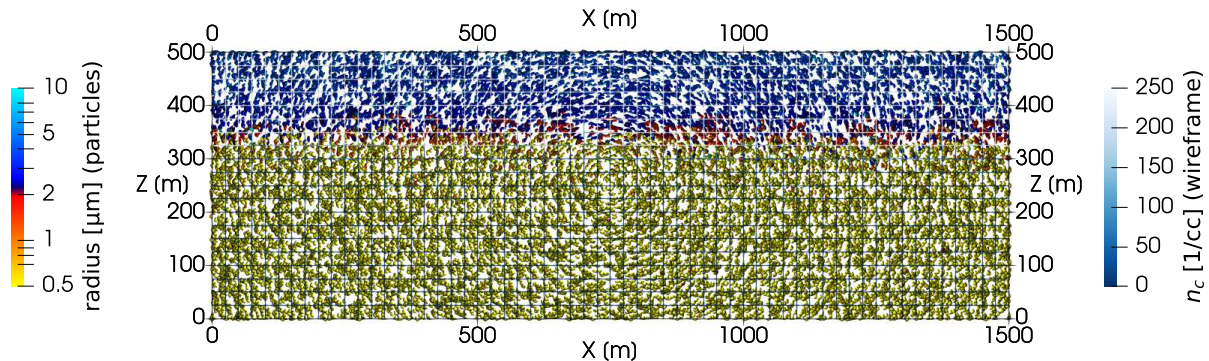
Time: 60 s (spin-up till 600.0 s)



16+16 super-particles/cell for INP-rich + INP-free particles

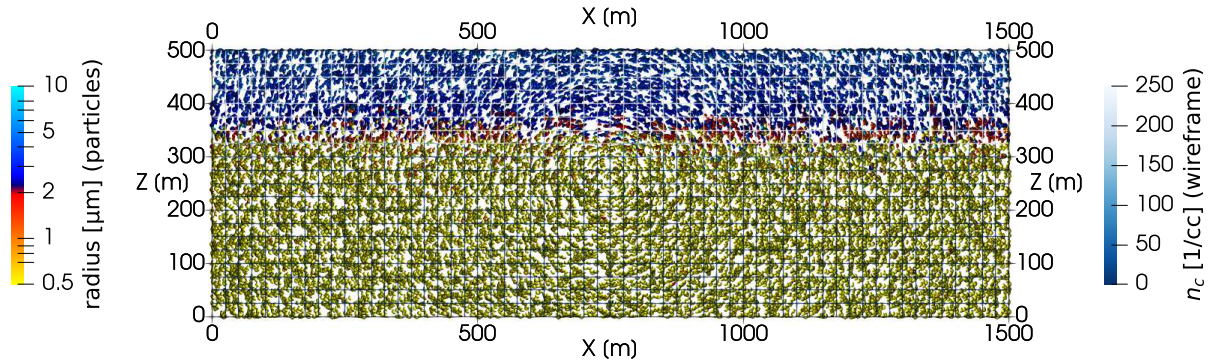
$N_{\text{aer}} = 300/\text{cc}$  (two-mode lognormal)    $N_{\text{INP}} = 150/L$  (lognormal,  $D_g = 0.74 \mu\text{m}$ ,  $\sigma_g = 2.55$ )  
spin-up = freezing off; subsequently frozen particles act as tracers

Time: 90 s (spin-up till 600.0 s)



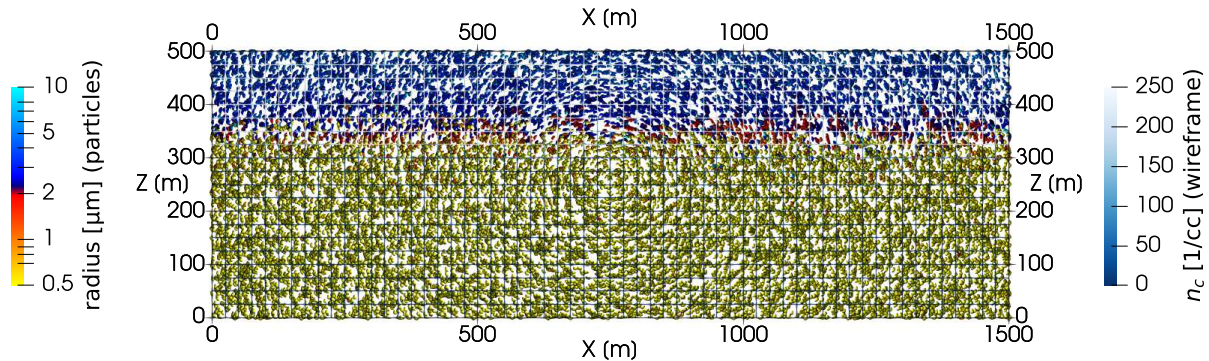
16+16 super-particles/cell for INP-rich + INP-free particles  
 $N_{\text{aer}} = 300/\text{cc}$  (two-mode lognormal)    $N_{\text{INP}} = 150/L$  (lognormal,  $D_g = 0.74 \mu\text{m}$ ,  $\sigma_g = 2.55$ )  
spin-up = freezing off; subsequently frozen particles act as tracers

Time: 120 s (spin-up till 600.0 s)



16+16 super-particles/cell for INP-rich + INP-free particles  
 $N_{\text{aer}} = 300/\text{cc}$  (two-mode lognormal)    $N_{\text{INP}} = 150/L$  (lognormal,  $D_g = 0.74 \mu\text{m}$ ,  $\sigma_g = 2.55$ )  
spin-up = freezing off; subsequently frozen particles act as tracers

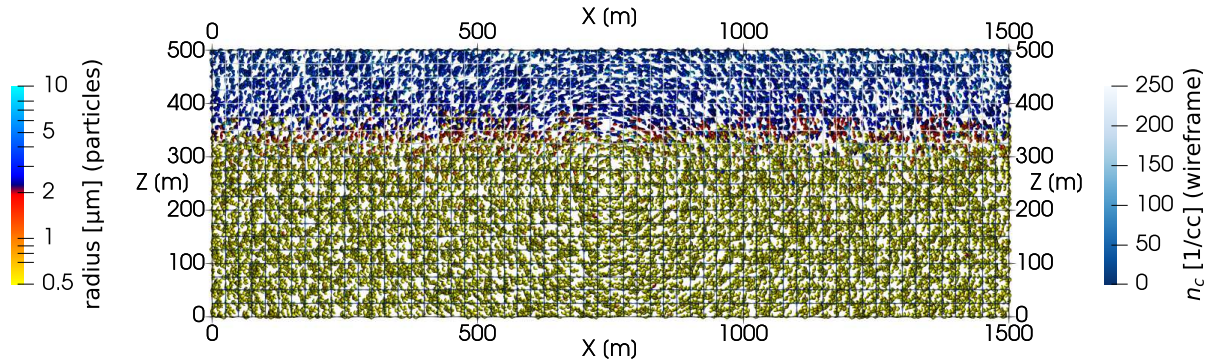
Time: 150 s (spin-up till 600.0 s)



16+16 super-particles/cell for INP-rich + INP-free particles

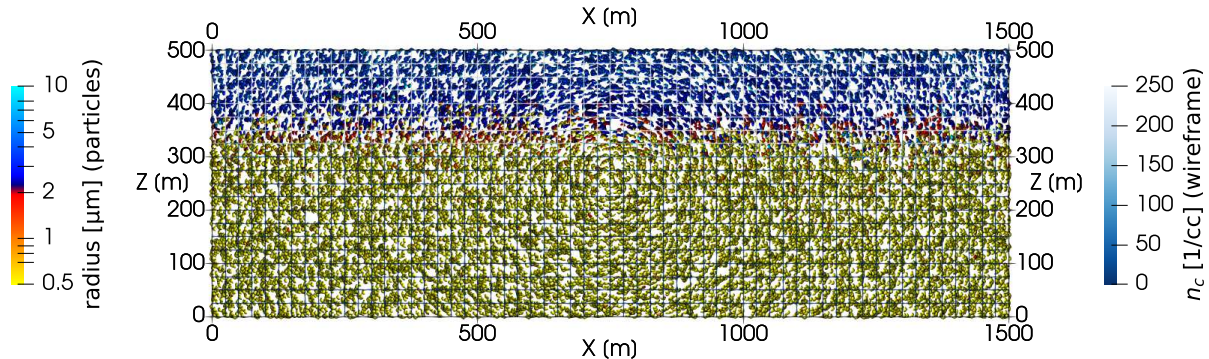
$N_{\text{aer}} = 300/\text{cc}$  (two-mode lognormal)     $N_{\text{INP}} = 150/L$  (lognormal,  $D_g = 0.74 \mu\text{m}$ ,  $\sigma_g = 2.55$ )  
spin-up = freezing off; subsequently frozen particles act as tracers

Time: 180 s (spin-up till 600.0 s)



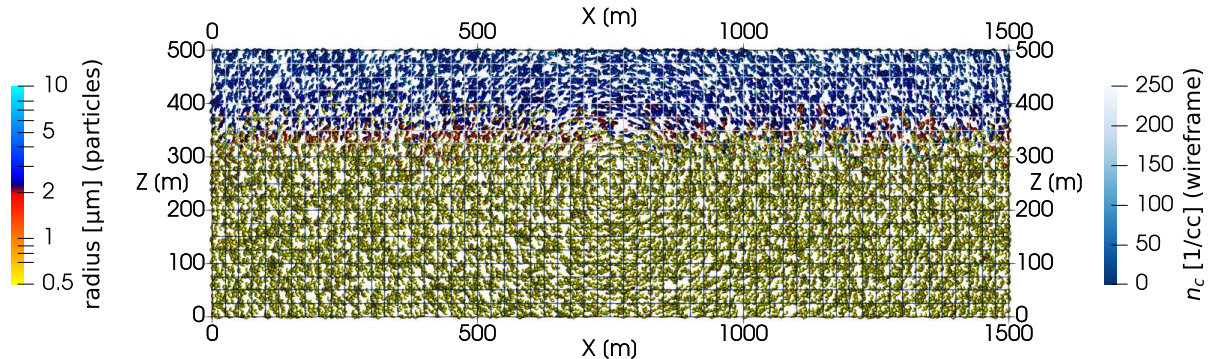
16+16 super-particles/cell for INP-rich + INP-free particles  
 $N_{\text{aer}} = 300/\text{cc}$  (two-mode lognormal)    $N_{\text{INP}} = 150/L$  (lognormal,  $D_g = 0.74 \mu\text{m}$ ,  $\sigma_g = 2.55$ )  
spin-up = freezing off; subsequently frozen particles act as tracers

Time: 210 s (spin-up till 600.0 s)



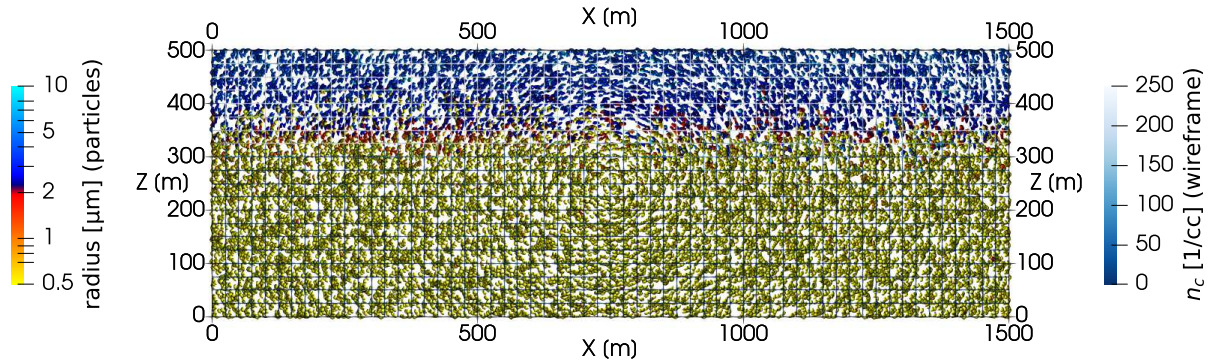
16+16 super-particles/cell for INP-rich + INP-free particles  
 $N_{\text{aer}} = 300/\text{cc}$  (two-mode lognormal)    $N_{\text{INP}} = 150/L$  (lognormal,  $D_g = 0.74 \mu\text{m}$ ,  $\sigma_g = 2.55$ )  
spin-up = freezing off; subsequently frozen particles act as tracers

Time: 240 s (spin-up till 600.0 s)



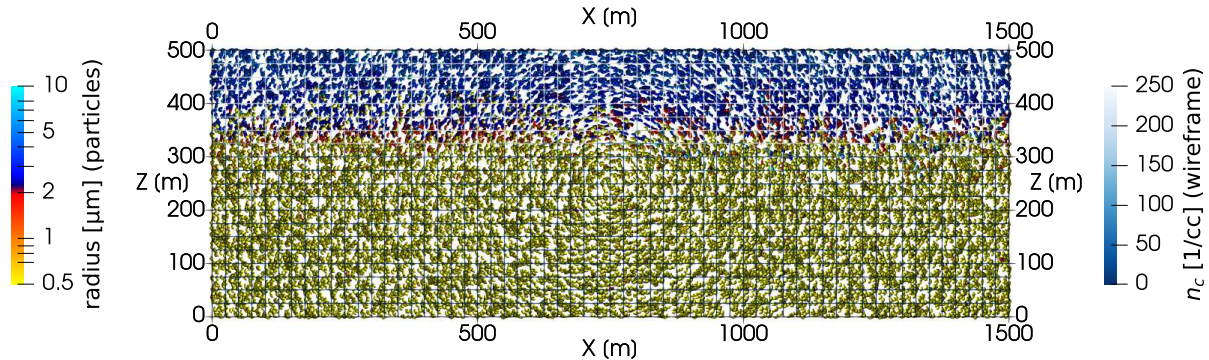
16+16 super-particles/cell for INP-rich + INP-free particles  
 $N_{\text{aer}} = 300/\text{cc}$  (two-mode lognormal)    $N_{\text{INP}} = 150/L$  (lognormal,  $D_g = 0.74 \mu\text{m}$ ,  $\sigma_g = 2.55$ )  
spin-up = freezing off; subsequently frozen particles act as tracers

Time: 270 s (spin-up till 600.0 s)



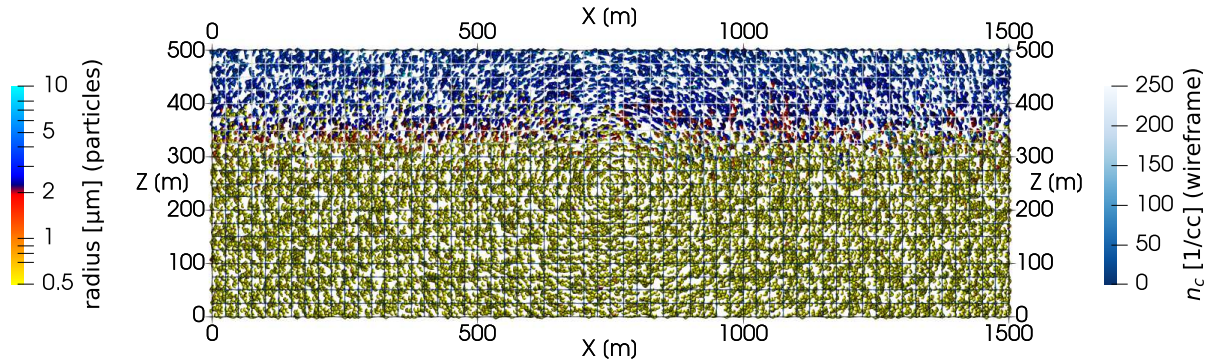
16+16 super-particles/cell for INP-rich + INP-free particles  
 $N_{\text{aer}} = 300/\text{cc}$  (two-mode lognormal)    $N_{\text{INP}} = 150/L$  (lognormal,  $D_g = 0.74 \mu\text{m}$ ,  $\sigma_g = 2.55$ )  
spin-up = freezing off; subsequently frozen particles act as tracers

Time: 300 s (spin-up till 600.0 s)



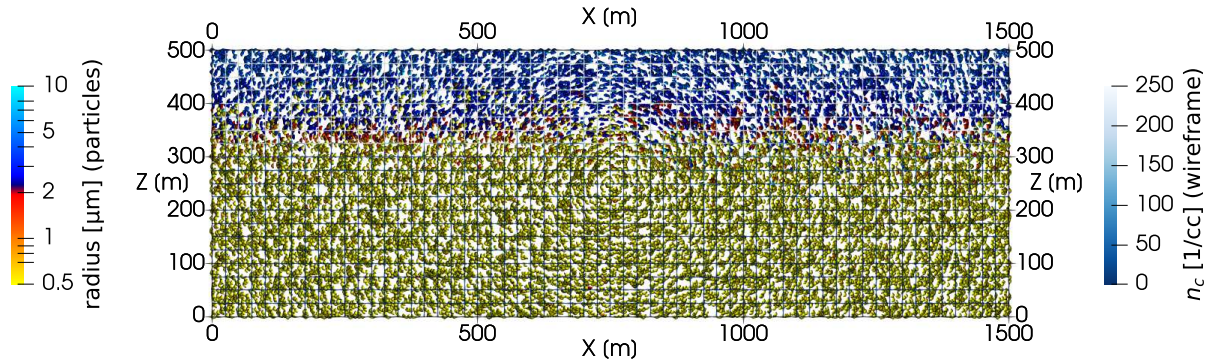
16+16 super-particles/cell for INP-rich + INP-free particles  
 $N_{\text{aer}} = 300/\text{cc}$  (two-mode lognormal)    $N_{\text{INP}} = 150/L$  (lognormal,  $D_g = 0.74 \mu\text{m}$ ,  $\sigma_g = 2.55$ )  
spin-up = freezing off; subsequently frozen particles act as tracers

Time: 330 s (spin-up till 600.0 s)



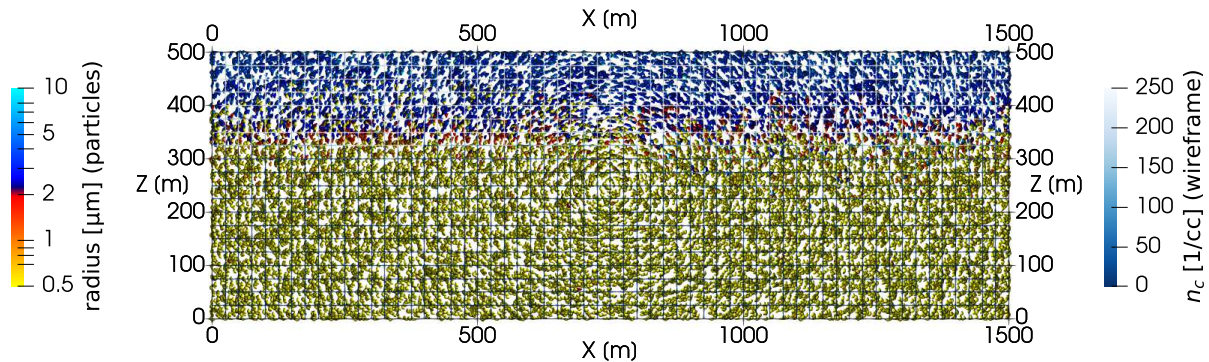
16+16 super-particles/cell for INP-rich + INP-free particles  
 $N_{\text{aer}} = 300/\text{cc}$  (two-mode lognormal)    $N_{\text{INP}} = 150/L$  (lognormal,  $D_g = 0.74 \mu\text{m}$ ,  $\sigma_g = 2.55$ )  
spin-up = freezing off; subsequently frozen particles act as tracers

Time: 360 s (spin-up till 600.0 s)



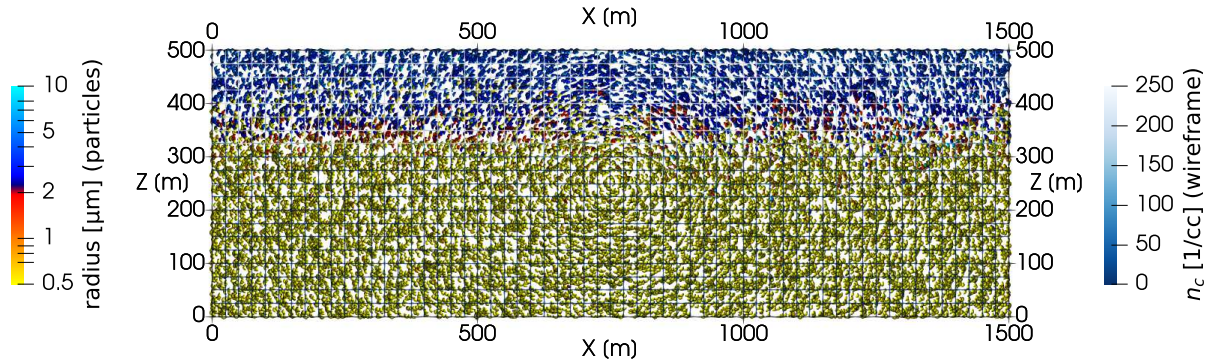
16+16 super-particles/cell for INP-rich + INP-free particles  
 $N_{\text{aer}} = 300/\text{cc}$  (two-mode lognormal)    $N_{\text{INP}} = 150/L$  (lognormal,  $D_g = 0.74 \mu\text{m}$ ,  $\sigma_g = 2.55$ )  
spin-up = freezing off; subsequently frozen particles act as tracers

Time: 390 s (spin-up till 600.0 s)



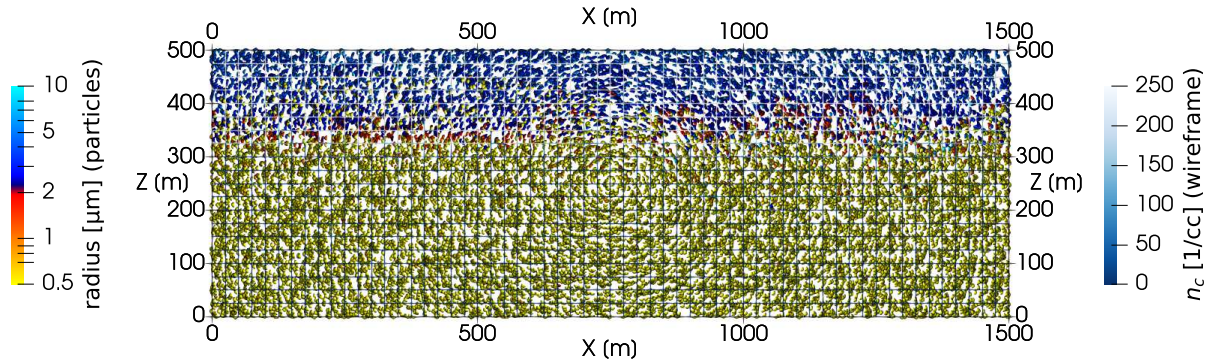
16+16 super-particles/cell for INP-rich + INP-free particles  
 $N_{\text{aer}} = 300/\text{cc}$  (two-mode lognormal)    $N_{\text{INP}} = 150/L$  (lognormal,  $D_g = 0.74 \mu\text{m}$ ,  $\sigma_g = 2.55$ )  
spin-up = freezing off; subsequently frozen particles act as tracers

Time: 420 s (spin-up till 600.0 s)



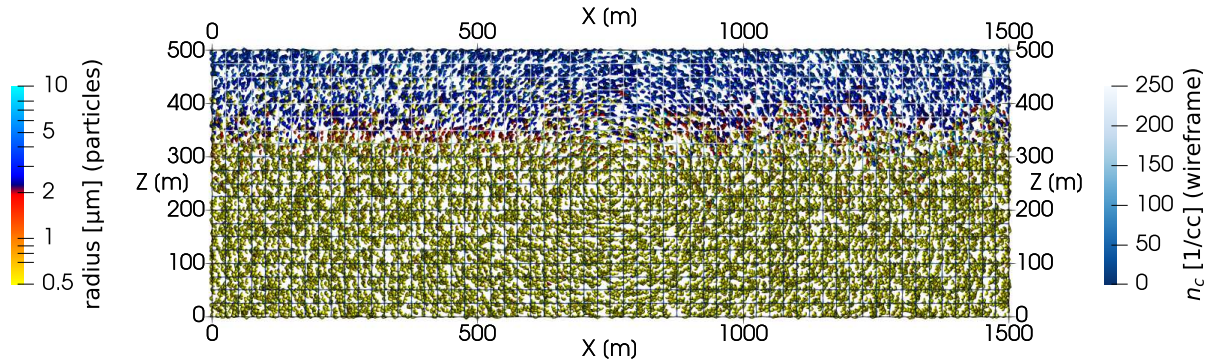
16+16 super-particles/cell for INP-rich + INP-free particles  
 $N_{\text{aer}} = 300/\text{cc}$  (two-mode lognormal)    $N_{\text{INP}} = 150/L$  (lognormal,  $D_g = 0.74 \mu\text{m}$ ,  $\sigma_g = 2.55$ )  
spin-up = freezing off; subsequently frozen particles act as tracers

Time: 450 s (spin-up till 600.0 s)



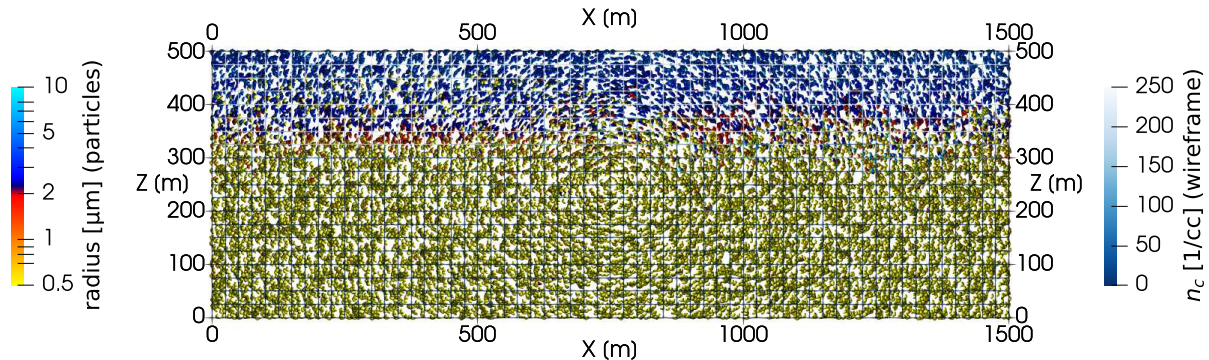
16+16 super-particles/cell for INP-rich + INP-free particles  
 $N_{\text{aer}} = 300/\text{cc}$  (two-mode lognormal)    $N_{\text{INP}} = 150/L$  (lognormal,  $D_g = 0.74 \mu\text{m}$ ,  $\sigma_g = 2.55$ )  
spin-up = freezing off; subsequently frozen particles act as tracers

Time: 480 s (spin-up till 600.0 s)



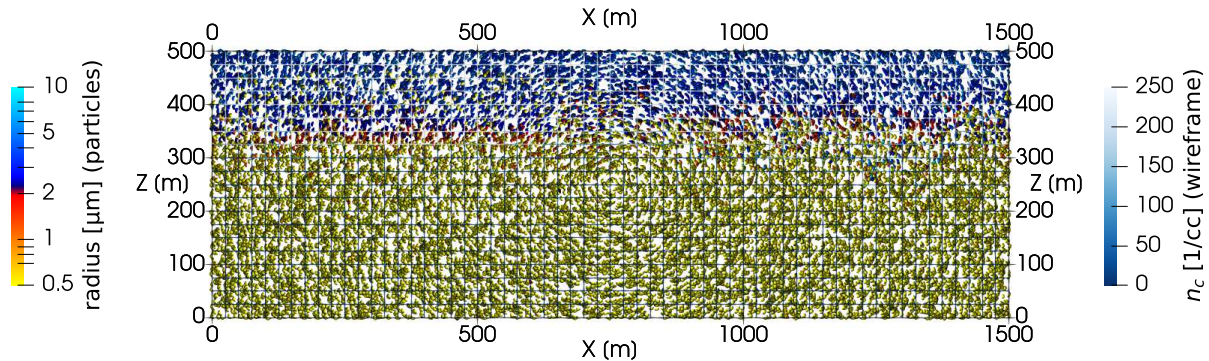
16+16 super-particles/cell for INP-rich + INP-free particles  
 $N_{\text{aer}} = 300/\text{cc}$  (two-mode lognormal)    $N_{\text{INP}} = 150/L$  (lognormal,  $D_g = 0.74 \mu\text{m}$ ,  $\sigma_g = 2.55$ )  
spin-up = freezing off; subsequently frozen particles act as tracers

Time: 510 s (spin-up till 600.0 s)



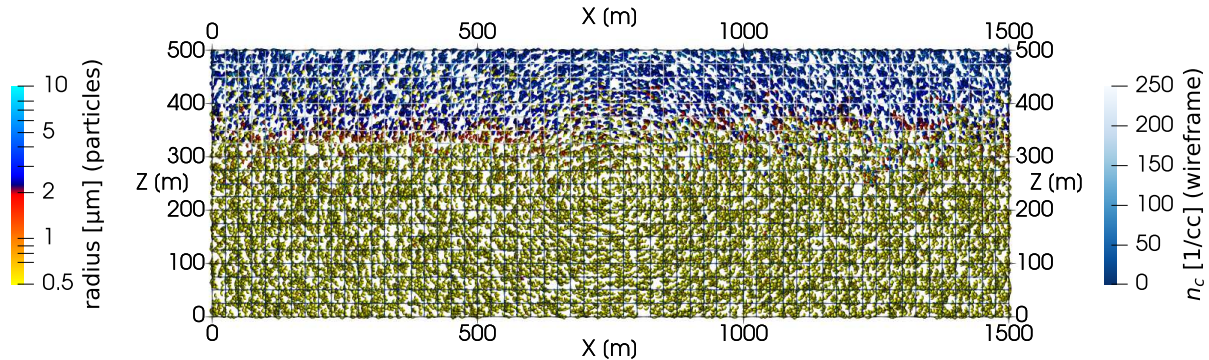
16+16 super-particles/cell for INP-rich + INP-free particles  
 $N_{\text{aer}} = 300/\text{cc}$  (two-mode lognormal)    $N_{\text{INP}} = 150/L$  (lognormal,  $D_g = 0.74 \mu\text{m}$ ,  $\sigma_g = 2.55$ )  
spin-up = freezing off; subsequently frozen particles act as tracers

Time: 540 s (spin-up till 600.0 s)



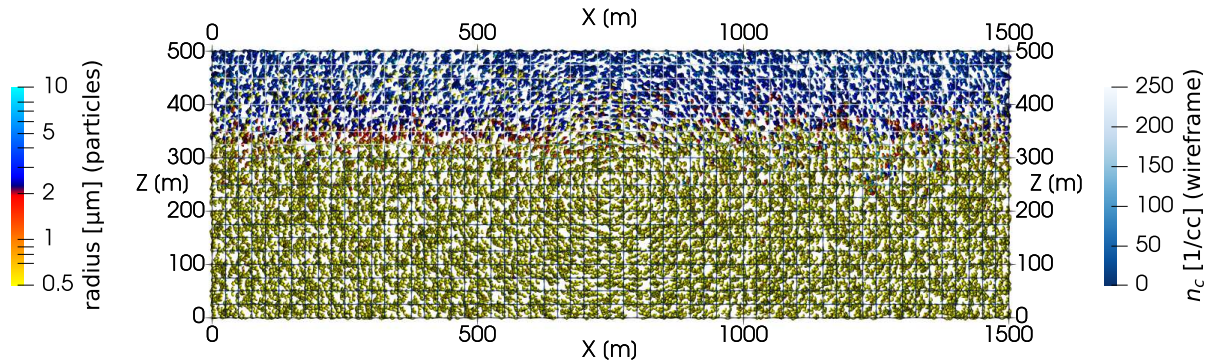
16+16 super-particles/cell for INP-rich + INP-free particles  
 $N_{\text{aer}} = 300/\text{cc}$  (two-mode lognormal)    $N_{\text{INP}} = 150/L$  (lognormal,  $D_g = 0.74 \mu\text{m}$ ,  $\sigma_g = 2.55$ )  
spin-up = freezing off; subsequently frozen particles act as tracers

Time: 570 s (spin-up till 600.0 s)



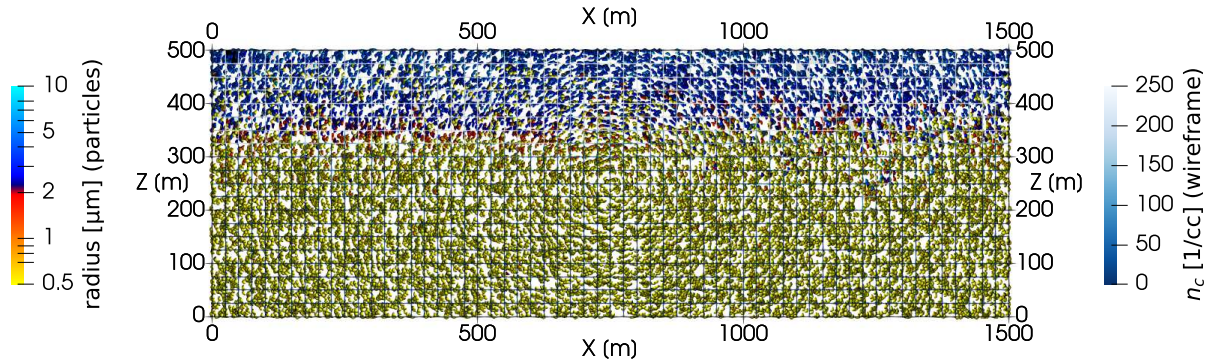
16+16 super-particles/cell for INP-rich + INP-free particles  
 $N_{\text{aer}} = 300/\text{cc}$  (two-mode lognormal)    $N_{\text{INP}} = 150/L$  (lognormal,  $D_g = 0.74 \mu\text{m}$ ,  $\sigma_g = 2.55$ )  
spin-up = freezing off; subsequently frozen particles act as tracers

Time: 600 s (spin-up till 600.0 s)



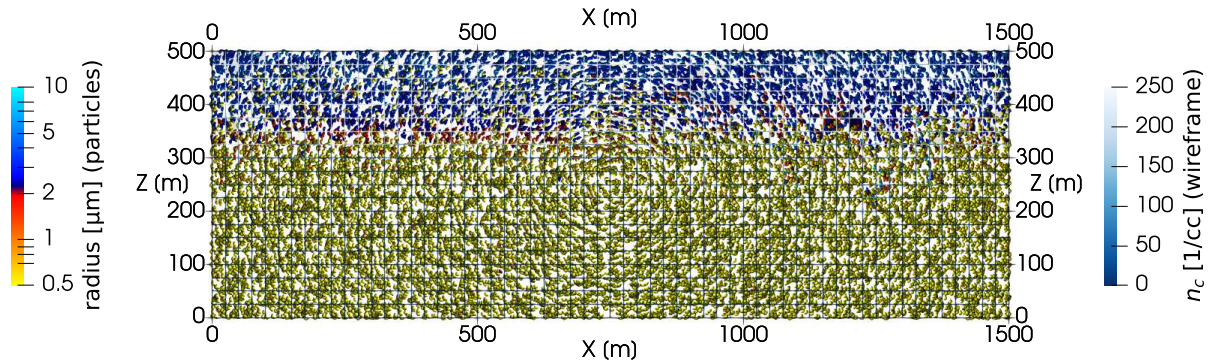
16+16 super-particles/cell for INP-rich + INP-free particles  
 $N_{\text{aer}} = 300/\text{cc}$  (two-mode lognormal)    $N_{\text{INP}} = 150/L$  (lognormal,  $D_g = 0.74 \mu\text{m}$ ,  $\sigma_g = 2.55$ )  
spin-up = freezing off; subsequently frozen particles act as tracers

Time: 630 s (spin-up till 600.0 s)



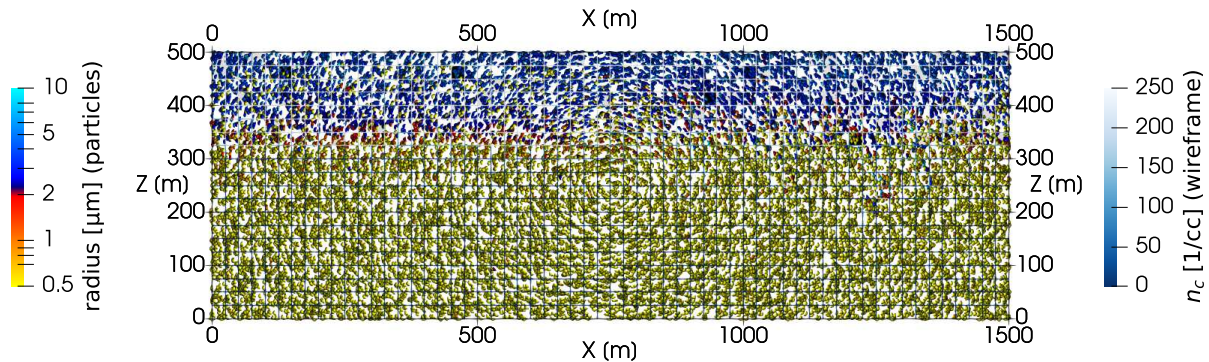
16+16 super-particles/cell for INP-rich + INP-free particles  
 $N_{\text{aer}} = 300/\text{cc}$  (two-mode lognormal)    $N_{\text{INP}} = 150/L$  (lognormal,  $D_g = 0.74 \mu\text{m}$ ,  $\sigma_g = 2.55$ )  
spin-up = freezing off; subsequently frozen particles act as tracers

Time: 660 s (spin-up till 600.0 s)



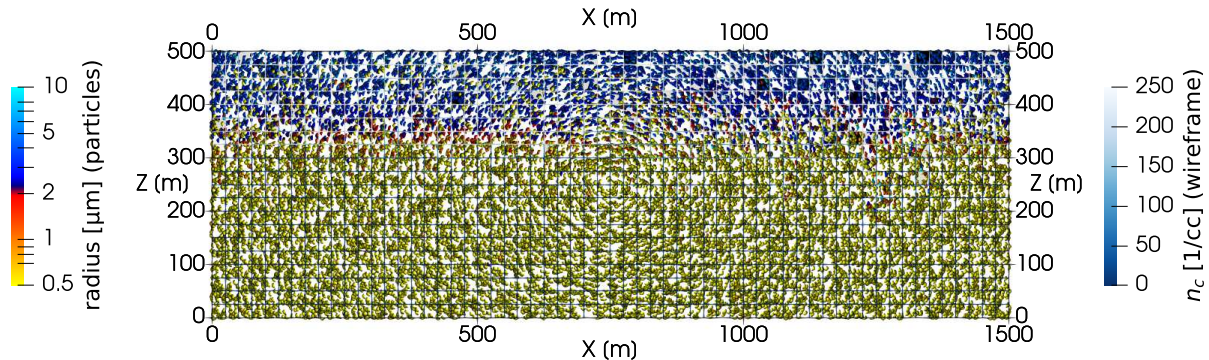
16+16 super-particles/cell for INP-rich + INP-free particles  
 $N_{\text{aer}} = 300/\text{cc}$  (two-mode lognormal)    $N_{\text{INP}} = 150/L$  (lognormal,  $D_g = 0.74 \mu\text{m}$ ,  $\sigma_g = 2.55$ )  
spin-up = freezing off; subsequently frozen particles act as tracers

Time: 690 s (spin-up till 600.0 s)



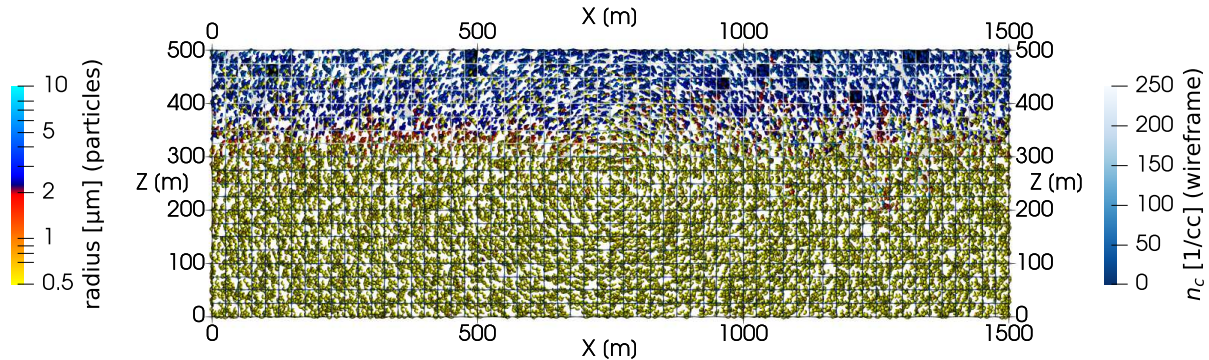
16+16 super-particles/cell for INP-rich + INP-free particles  
 $N_{\text{aer}} = 300/\text{cc}$  (two-mode lognormal)    $N_{\text{INP}} = 150/L$  (lognormal,  $D_g = 0.74 \mu\text{m}$ ,  $\sigma_g = 2.55$ )  
spin-up = freezing off; subsequently frozen particles act as tracers

Time: 720 s (spin-up till 600.0 s)



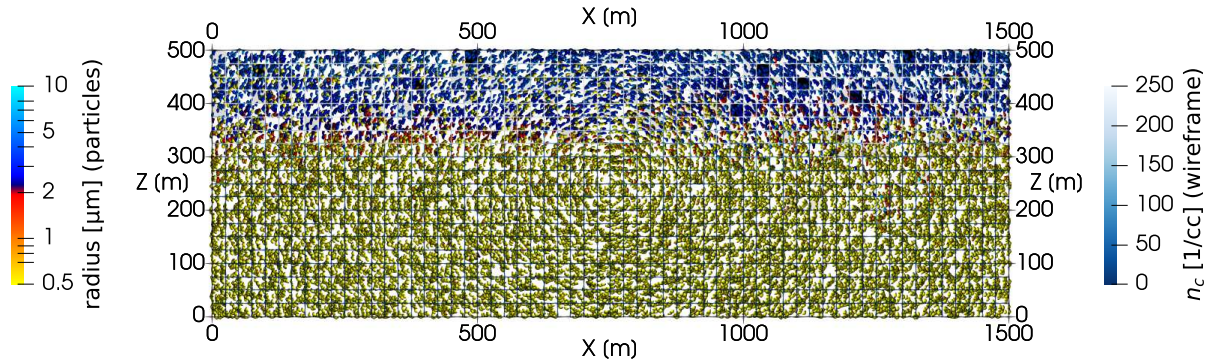
16+16 super-particles/cell for INP-rich + INP-free particles  
 $N_{\text{aer}} = 300/\text{cc}$  (two-mode lognormal)    $N_{\text{INP}} = 150/L$  (lognormal,  $D_g = 0.74 \mu\text{m}$ ,  $\sigma_g = 2.55$ )  
spin-up = freezing off; subsequently frozen particles act as tracers

Time: 750 s (spin-up till 600.0 s)



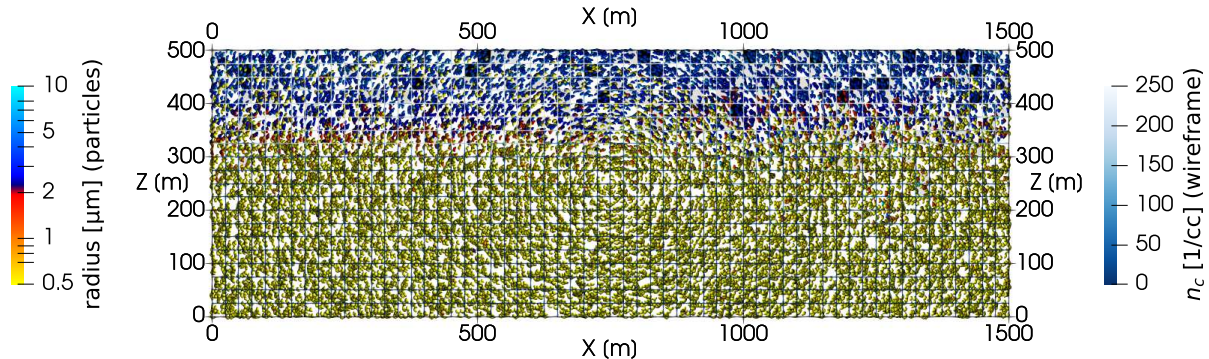
16+16 super-particles/cell for INP-rich + INP-free particles  
 $N_{\text{aer}} = 300/\text{cc}$  (two-mode lognormal)    $N_{\text{INP}} = 150/L$  (lognormal,  $D_g = 0.74 \mu\text{m}$ ,  $\sigma_g = 2.55$ )  
spin-up = freezing off; subsequently frozen particles act as tracers

Time: 780 s (spin-up till 600.0 s)



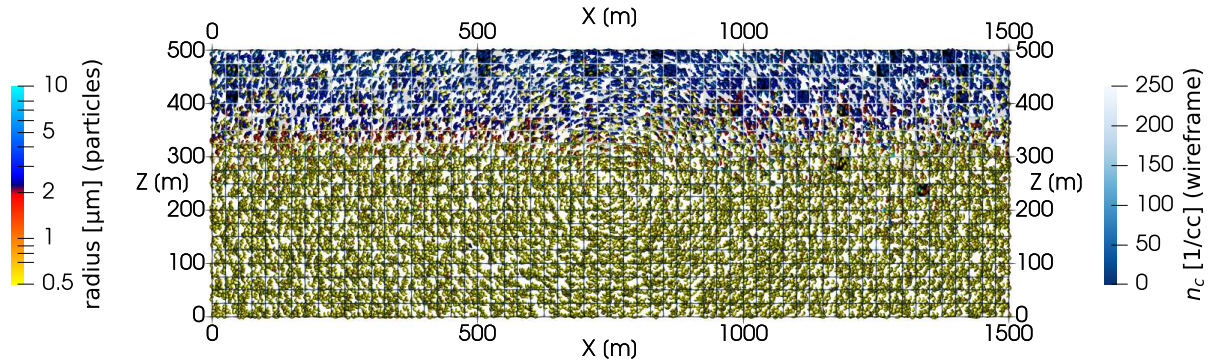
16+16 super-particles/cell for INP-rich + INP-free particles  
 $N_{\text{aer}} = 300/\text{cc}$  (two-mode lognormal)    $N_{\text{INP}} = 150/L$  (lognormal,  $D_g = 0.74 \mu\text{m}$ ,  $\sigma_g = 2.55$ )  
spin-up = freezing off; subsequently frozen particles act as tracers

Time: 810 s (spin-up till 600.0 s)



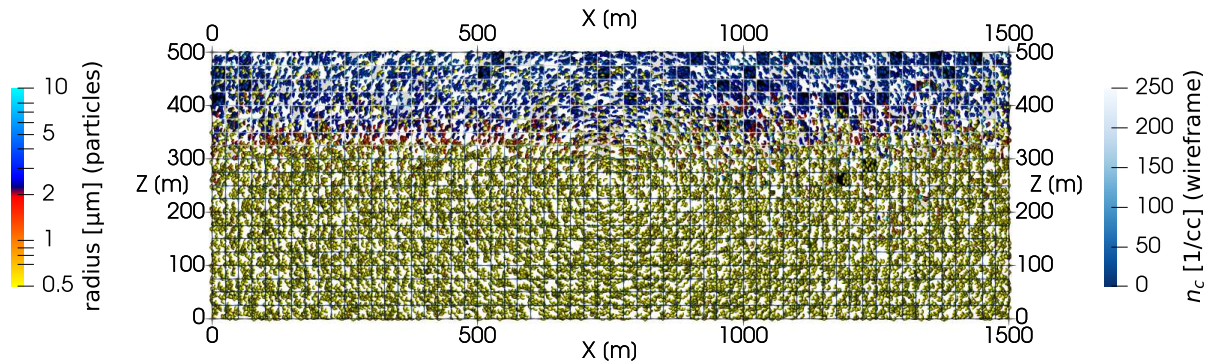
16+16 super-particles/cell for INP-rich + INP-free particles  
 $N_{\text{aer}} = 300/\text{cc}$  (two-mode lognormal)    $N_{\text{INP}} = 150/L$  (lognormal,  $D_g = 0.74 \mu\text{m}$ ,  $\sigma_g = 2.55$ )  
spin-up = freezing off; subsequently frozen particles act as tracers

Time: 840 s (spin-up till 600.0 s)



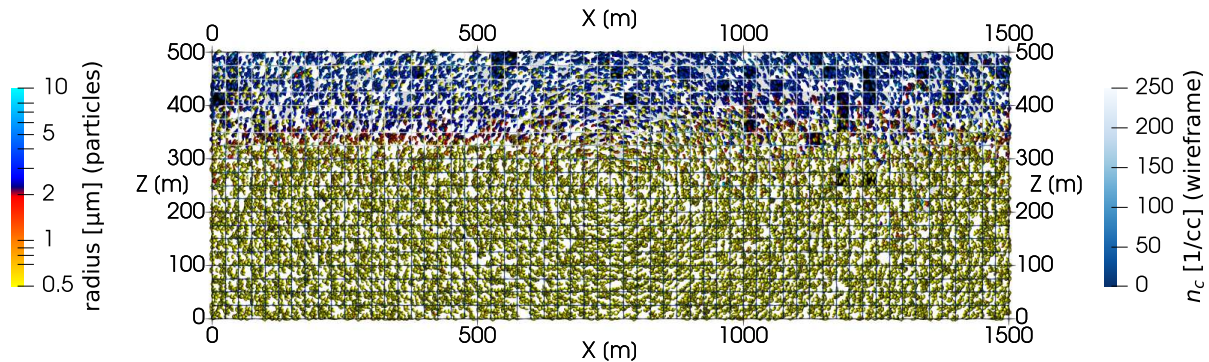
16+16 super-particles/cell for INP-rich + INP-free particles  
 $N_{\text{aer}} = 300/\text{cc}$  (two-mode lognormal)    $N_{\text{INP}} = 150/L$  (lognormal,  $D_g = 0.74 \mu\text{m}$ ,  $\sigma_g = 2.55$ )  
spin-up = freezing off; subsequently frozen particles act as tracers

Time: 870 s (spin-up till 600.0 s)



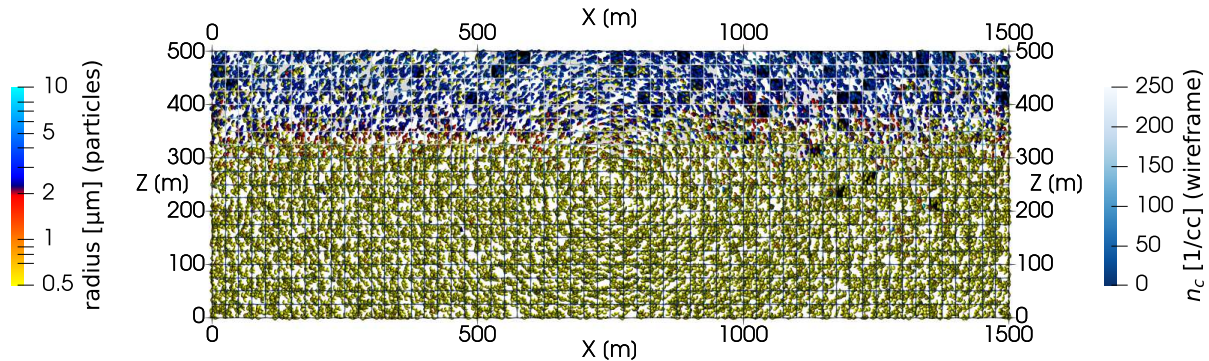
16+16 super-particles/cell for INP-rich + INP-free particles  
 $N_{\text{aer}} = 300/\text{cc}$  (two-mode lognormal)    $N_{\text{INP}} = 150/L$  (lognormal,  $D_g = 0.74 \mu\text{m}$ ,  $\sigma_g = 2.55$ )  
spin-up = freezing off; subsequently frozen particles act as tracers

Time: 900 s (spin-up till 600.0 s)



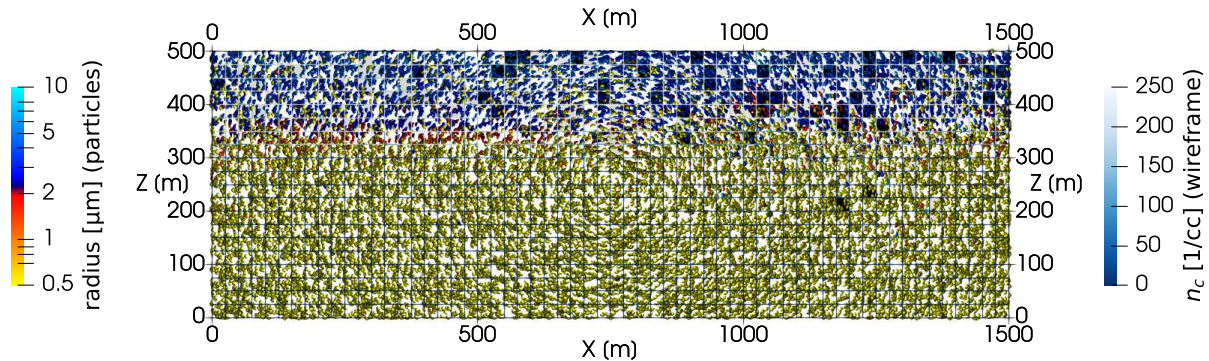
16+16 super-particles/cell for INP-rich + INP-free particles  
 $N_{\text{aer}} = 300/\text{cc}$  (two-mode lognormal)    $N_{\text{INP}} = 150/L$  (lognormal,  $D_g = 0.74 \mu\text{m}$ ,  $\sigma_g = 2.55$ )  
spin-up = freezing off; subsequently frozen particles act as tracers

Time: 930 s (spin-up till 600.0 s)



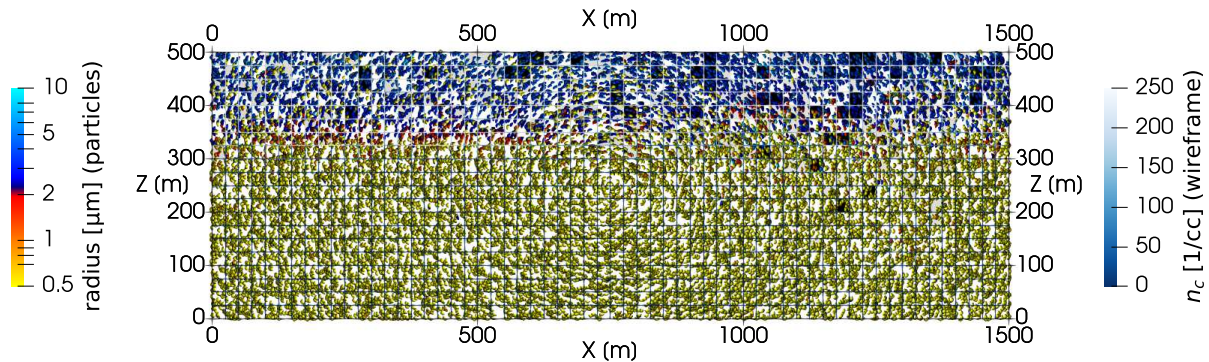
16+16 super-particles/cell for INP-rich + INP-free particles  
 $N_{\text{aer}} = 300/\text{cc}$  (two-mode lognormal)    $N_{\text{INP}} = 150/L$  (lognormal,  $D_g = 0.74 \mu\text{m}$ ,  $\sigma_g = 2.55$ )  
spin-up = freezing off; subsequently frozen particles act as tracers

Time: 960 s (spin-up till 600.0 s)



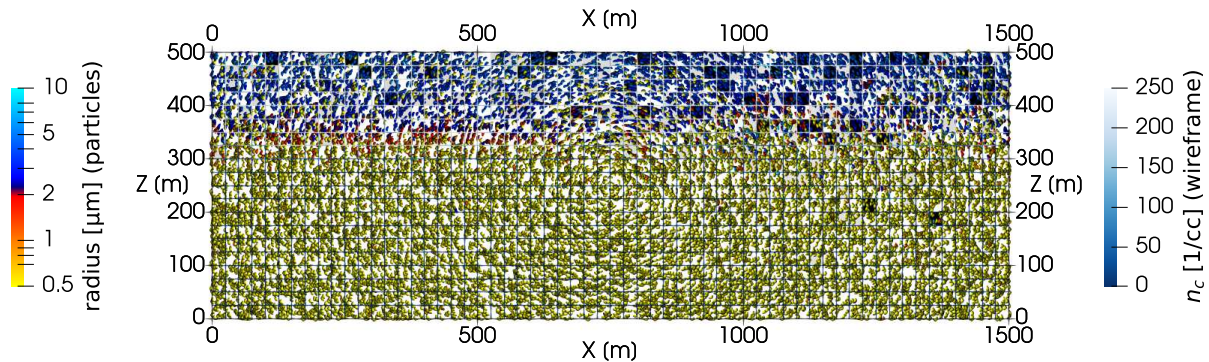
16+16 super-particles/cell for INP-rich + INP-free particles  
 $N_{\text{aer}} = 300/\text{cc}$  (two-mode lognormal)    $N_{\text{INP}} = 150/L$  (lognormal,  $D_g = 0.74 \mu\text{m}$ ,  $\sigma_g = 2.55$ )  
spin-up = freezing off; subsequently frozen particles act as tracers

Time: 990 s (spin-up till 600.0 s)



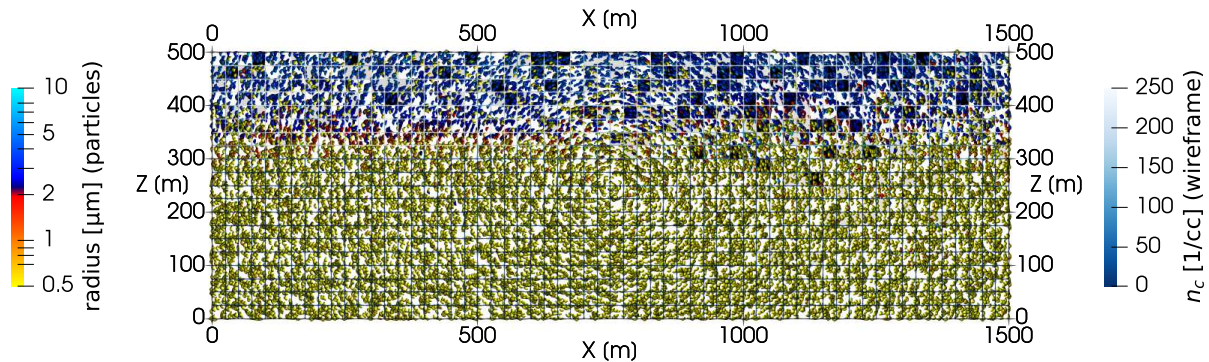
16+16 super-particles/cell for INP-rich + INP-free particles  
 $N_{\text{aer}} = 300/\text{cc}$  (two-mode lognormal)    $N_{\text{INP}} = 150/L$  (lognormal,  $D_g = 0.74 \mu\text{m}$ ,  $\sigma_g = 2.55$ )  
spin-up = freezing off; subsequently frozen particles act as tracers

Time: 1020 s (spin-up till 600.0 s)



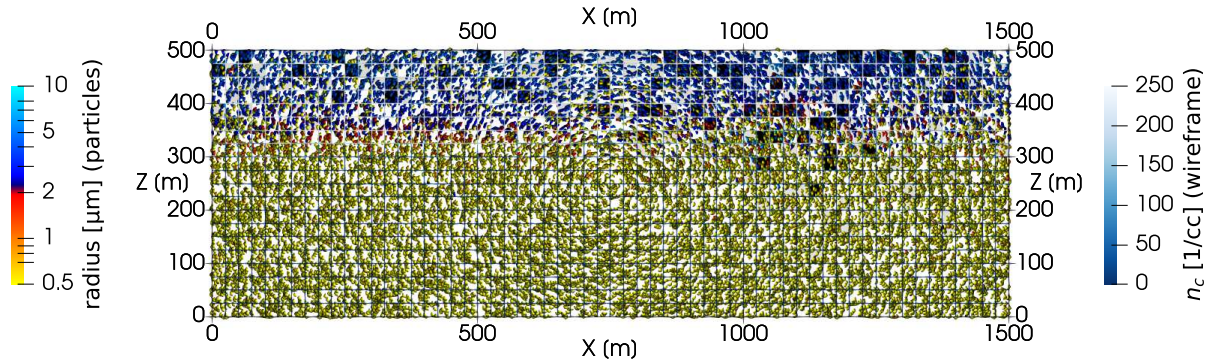
16+16 super-particles/cell for INP-rich + INP-free particles  
 $N_{\text{aer}} = 300/\text{cc}$  (two-mode lognormal)    $N_{\text{INP}} = 150/L$  (lognormal,  $D_g = 0.74 \mu\text{m}$ ,  $\sigma_g = 2.55$ )  
spin-up = freezing off; subsequently frozen particles act as tracers

Time: 1050 s (spin-up till 600.0 s)



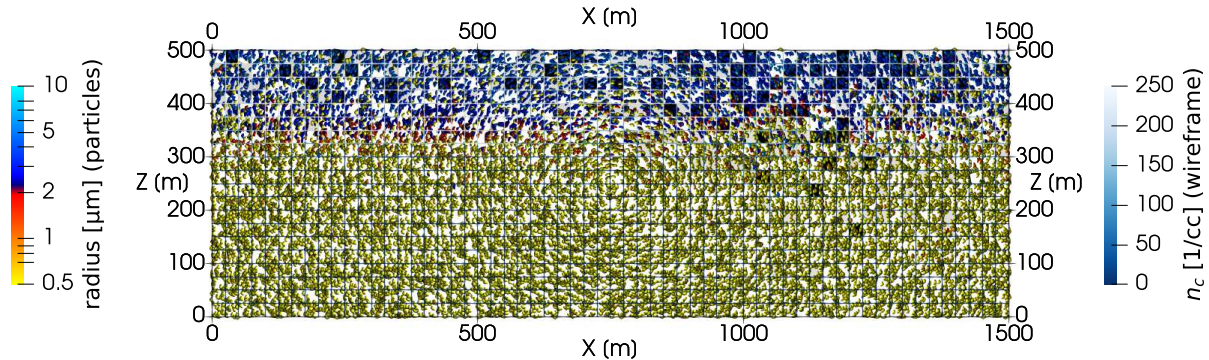
16+16 super-particles/cell for INP-rich + INP-free particles  
 $N_{\text{aer}} = 300/\text{cc}$  (two-mode lognormal)    $N_{\text{INP}} = 150/L$  (lognormal,  $D_g = 0.74 \mu\text{m}$ ,  $\sigma_g = 2.55$ )  
spin-up = freezing off; subsequently frozen particles act as tracers

Time: 1080 s (spin-up till 600.0 s)



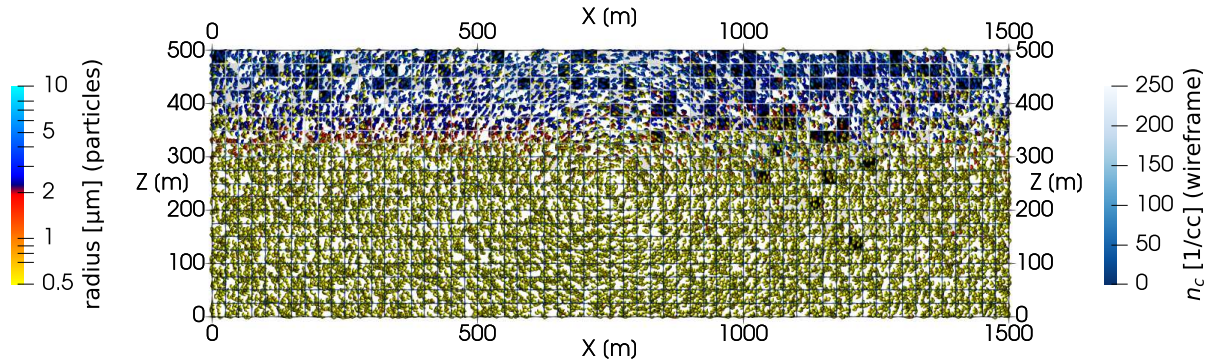
16+16 super-particles/cell for INP-rich + INP-free particles  
 $N_{\text{aer}} = 300/\text{cc}$  (two-mode lognormal)    $N_{\text{INP}} = 150/L$  (lognormal,  $D_g = 0.74 \mu\text{m}$ ,  $\sigma_g = 2.55$ )  
spin-up = freezing off; subsequently frozen particles act as tracers

Time: 1110 s (spin-up till 600.0 s)



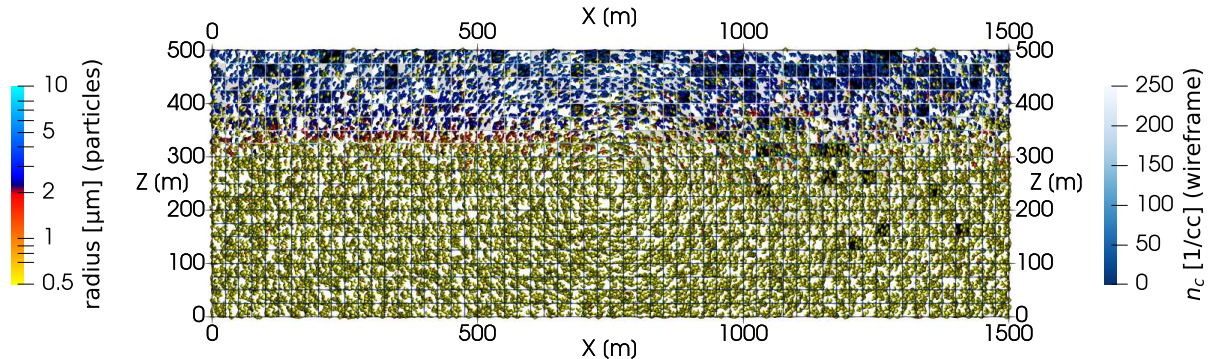
16+16 super-particles/cell for INP-rich + INP-free particles  
 $N_{\text{aer}} = 300/\text{cc}$  (two-mode lognormal)    $N_{\text{INP}} = 150/L$  (lognormal,  $D_g = 0.74 \mu\text{m}$ ,  $\sigma_g = 2.55$ )  
spin-up = freezing off; subsequently frozen particles act as tracers

Time: 1140 s (spin-up till 600.0 s)



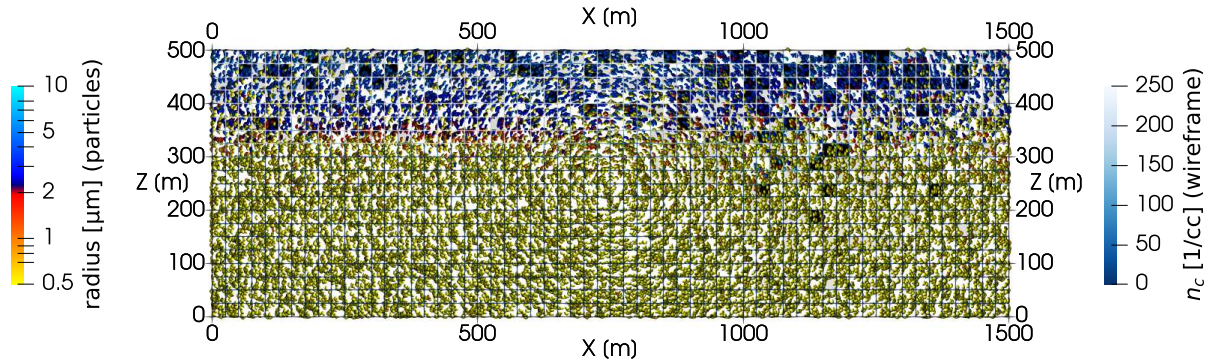
16+16 super-particles/cell for INP-rich + INP-free particles  
 $N_{\text{aer}} = 300/\text{cc}$  (two-mode lognormal)    $N_{\text{INP}} = 150/L$  (lognormal,  $D_g = 0.74 \mu\text{m}$ ,  $\sigma_g = 2.55$ )  
spin-up = freezing off; subsequently frozen particles act as tracers

Time: 1170 s (spin-up till 600.0 s)

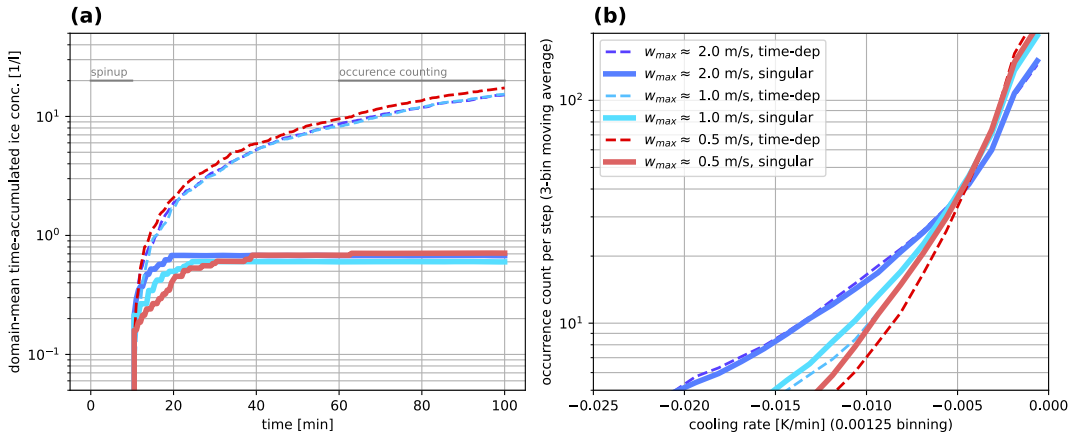


16+16 super-particles/cell for INP-rich + INP-free particles  
 $N_{\text{aer}} = 300/\text{cc}$  (two-mode lognormal)    $N_{\text{INP}} = 150/L$  (lognormal,  $D_g = 0.74 \mu\text{m}$ ,  $\sigma_g = 2.55$ )  
spin-up = freezing off; subsequently frozen particles act as tracers

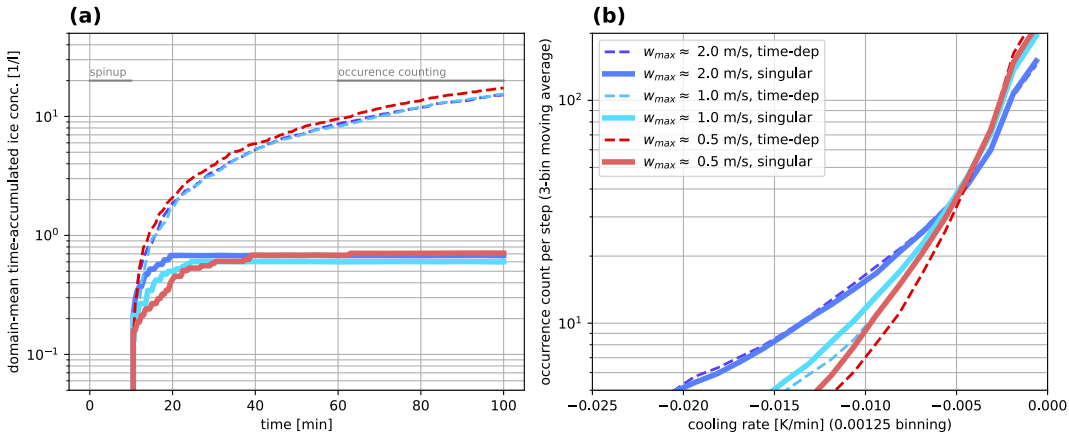
Time: 1200 s (spin-up till 600.0 s)



16+16 super-particles/cell for INP-rich + INP-free particles  
 $N_{\text{aer}} = 300/\text{cc}$  (two-mode lognormal)    $N_{\text{INP}} = 150/L$  (lognormal,  $D_g = 0.74 \mu\text{m}$ ,  $\sigma_g = 2.55$ )  
spin-up = freezing off; subsequently frozen particles act as tracers



- ▶ singular vs. time-dependent markedly different  
(consistent with box model for  $c \ll 1K/min$ )



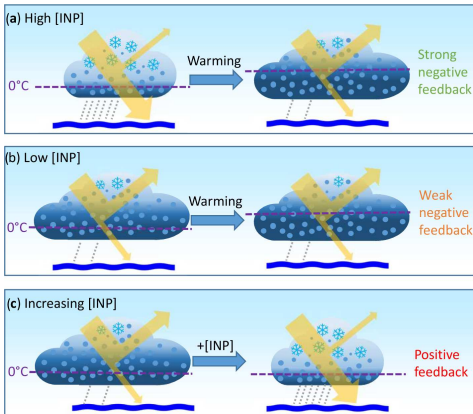
- ▶ singular vs. time-dependent markedly different  
(consistent with box model for  $c \ll 1K/min$ )
- ▶ range of cooling rates in simple flow  
(far from  $c \sim 1$  K/min for AIDA as in Niemand et al. 2012)

# Opinion: Cloud-phase climate feedback and the importance of ice-nucleating particles

Benjamin J. Murray<sup>1</sup>, Kenneth S. Carslaw<sup>1</sup>, and Paul R. Field<sup>1,2</sup>



Atmos. Chem. Phys., 21, 665–679, 2021  
<https://doi.org/10.5194/acp-21-665-2021>



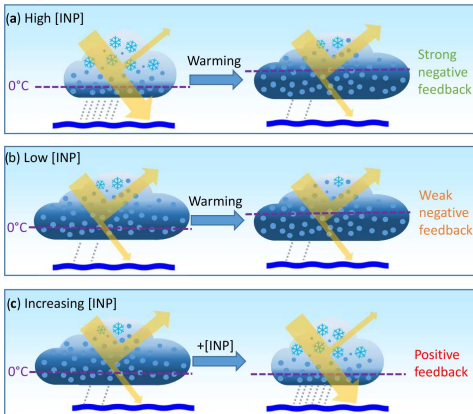
- ▶ *"it is becoming very clear that the cloud-phase feedback contributes substantially to the uncertainty in predictions of the rate at which our planet will warm in response to CO<sub>2</sub> emissions"*

# Opinion: Cloud-phase climate feedback and the importance of ice-nucleating particles

Benjamin J. Murray<sup>1</sup>, Kenneth S. Carslaw<sup>1</sup>, and Paul R. Field<sup>1,2</sup>

Atmospheric  
Chemistry  
and Physics  
Open Access  


Atmos. Chem. Phys., 21, 665–679, 2021  
<https://doi.org/10.5194/acp-21-665-2021>



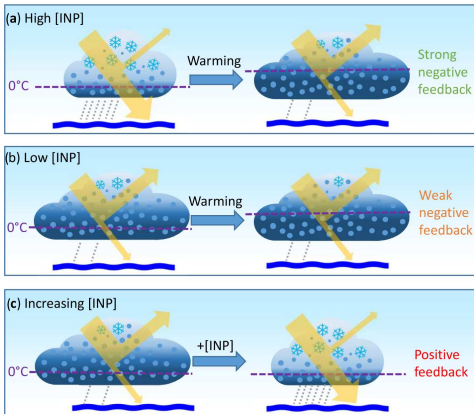
- ▶ *"it is becoming very clear that the cloud-phase feedback contributes substantially to the uncertainty in predictions of the rate at which our planet will warm in response to CO<sub>2</sub> emissions"*
- ▶ *"core physical process that drives the cloud-phase feedback is the transition to clouds with more liquid water and less ice as the isotherms shift upwards in a warmer world"*

# Opinion: Cloud-phase climate feedback and the importance of ice-nucleating particles

Benjamin J. Murray<sup>1</sup>, Kenneth S. Carslaw<sup>1</sup>, and Paul R. Field<sup>1,2</sup>

Atmospheric  
Chemistry  
and Physics  
Open Access  


Atmos. Chem. Phys., 21, 665–679, 2021  
<https://doi.org/10.5194/acp-21-665-2021>



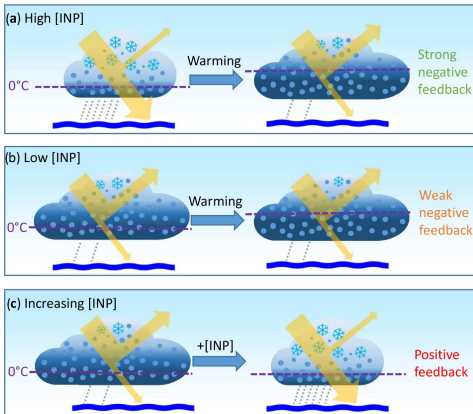
- ▶ *"it is becoming very clear that the cloud-phase feedback contributes substantially to the uncertainty in predictions of the rate at which our planet will warm in response to CO<sub>2</sub> emissions"*
- ▶ *"core physical process that drives the cloud-phase feedback is the transition to clouds with more liquid water and less ice as the isotherms shift upwards in a warmer world"*
- ▶ *"models need to improve their representation of ice-related microphysical processes; in particular, they need to include a direct link to aerosol type, specifically INPs"*

# Opinion: Cloud-phase climate feedback and the importance of ice-nucleating particles

Benjamin J. Murray<sup>1</sup>, Kenneth S. Carslaw<sup>1</sup>, and Paul R. Field<sup>1,2</sup>

Atmospheric  
Chemistry  
and Physics  
Open Access  

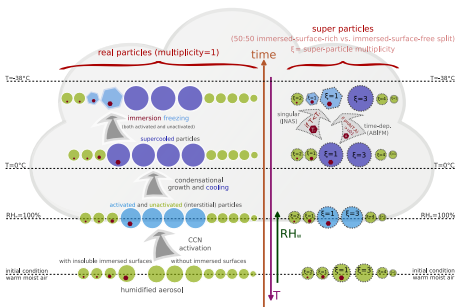

Atmos. Chem. Phys., 21, 665–679, 2021  
<https://doi.org/10.5194/acp-21-665-2021>

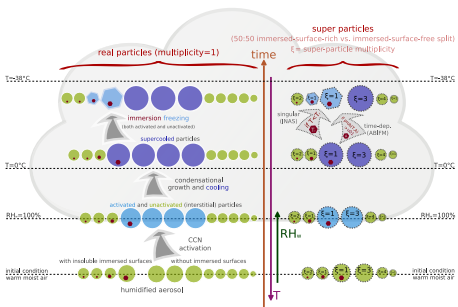
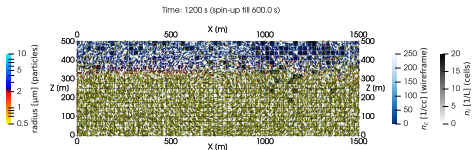


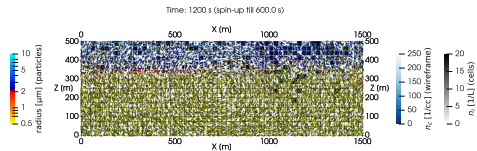
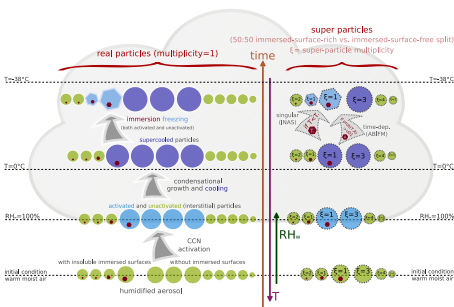
- ▶ *"it is becoming very clear that the cloud-phase feedback contributes substantially to the uncertainty in predictions of the rate at which our planet will warm in response to CO<sub>2</sub> emissions"*
- ▶ *"core physical process that drives the cloud-phase feedback is the transition to clouds with more liquid water and less ice as the isotherms shift upwards in a warmer world"*
- ▶ *"models need to improve their representation of ice-related microphysical processes; in particular, they need to include a direct link to aerosol type, specifically INPs"*
- ▶ *"must also represent the INP removal processes, which in turn depend on a correct representation of the microphysics"*











## RESEARCH TOPICS OFFERED BY THE AGH DOCTORAL SCHOOL IN THE ACADEMIC YEAR 2023/2024

If you wish to find research topics related to the area of your interest, type a few keywords into the search box and click the Search button. The general search explores complete topic descriptions and returns topics that contain all the provided words. If you want to limit your search to some of the table columns use the search boxes below the corresponding column labels. You can also sort the data by clicking the table headers.

Search for:

**Search**

**Clear filter**

Topic ID	Research topic	Faculty	Supervisor	Leading discipline	Funding source
1202	Modelling of isotopic signatures in precipitation using particle-based cloud microphysics	Faculty of Physics and Applied Computer Science	dr hab. inż. Miroslaw Zimnoch	physical sciences	Subsidy

## RESEARCH TOPICS OFFERED BY THE AGH DOCTORAL SCHOOL IN THE ACADEMIC YEAR 2023/2024

If you wish to find research topics related to the area of your interest, type a few keywords into the search box and click the Search button. The general search explores complete topic descriptions and returns topics that contain all the provided words. If you want to limit your search to some of the table columns use the search boxes below the corresponding column labels. You can also sort the data by clicking the table headers.

Search for:

Topic ID	Research topic	Faculty	Supervisor	Leading discipline	Funding source
1202	Modelling of isotopic signatures in precipitation using particle-based cloud microphysics	Faculty of Physics and Applied Computer Science	dr hab. inż. Miroslaw Zimnoch	physical sciences	Subsidy



## RESEARCH TOPICS OFFERED BY THE AGH DOCTORAL SCHOOL IN THE ACADEMIC YEAR 2023/2024

If you wish to find research topics related to the area of your interest, type a few keywords into the search box and click the Search button. The general search explores complete topic descriptions and returns topics that contain all the provided words. If you want to limit your search to some of the table columns use the search boxes below the corresponding column labels. You can also sort the data by clicking the table headers.

Search for:

**Search**

**Clear filter**

Topic ID	Research topic	Faculty	Supervisor	Leading discipline	Funding source
1202	Modelling of isotopic signatures in precipitation using particle-based cloud microphysics	Faculty of Physics and Applied Computer Science	dr hab. inż. Miroslaw Zimnoch	physical sciences	Subsidy

## RESEARCH TOPICS OFFERED BY THE AGH DOCTORAL SCHOOL IN THE ACADEMIC YEAR 2023/2024

If you wish to find research topics related to the area of your interest, type a few keywords into the search box and click the Search button. The general search explores complete topic descriptions and returns topics that contain all the provided words. If you want to limit your search to some of the table columns use the search boxes below the corresponding column labels. You can also sort the data by clicking the table headers.

Search for:

**Search**

**Clear filter**

Topic ID	Research topic	Faculty	Supervisor	Leading discipline	Funding source
1202	Modelling of isotopic signatures in precipitation using particle-based cloud microphysics	Faculty of Physics and Applied Computer Science	dr hab. inż. Miroslaw Zimnoch	physical sciences	Subsidy

## RESEARCH TOPICS OFFERED BY THE AGH DOCTORAL SCHOOL IN THE ACADEMIC YEAR 2023/2024

If you wish to find research topics related to the area of your interest, type a few keywords into the search box and click the Search button. The general search explores complete topic descriptions and returns topics that contain all the provided words. If you want to limit your search to some of the table columns use the search boxes below the corresponding column labels. You can also sort the data by clicking the table headers.

Search for:

**Search**

**Clear filter**

Topic ID	Research topic	Faculty	Supervisor	Leading discipline	Funding source
1202	Modelling of isotopic signatures in precipitation using particle-based cloud microphysics	Faculty of Physics and Applied Computer Science	dr hab. inż. Miroslaw Zimnoch	physical sciences	Subsidy